XVth Workshop on Aircraft Aerodynamics and Flight Dynamics
Central Aero-Hydrodynamics Institute n.a. Prof. N.E. Zhoukovsky (TsAGI)
Volodarskogo, Moscow Region, Russia, February 26-27, 2004

Author’s Translation from Russian

A Technique For Construction and Analysis Of Aircraft Flight Safety ‘Topology’ In Complex (Multi-Factor) Situations

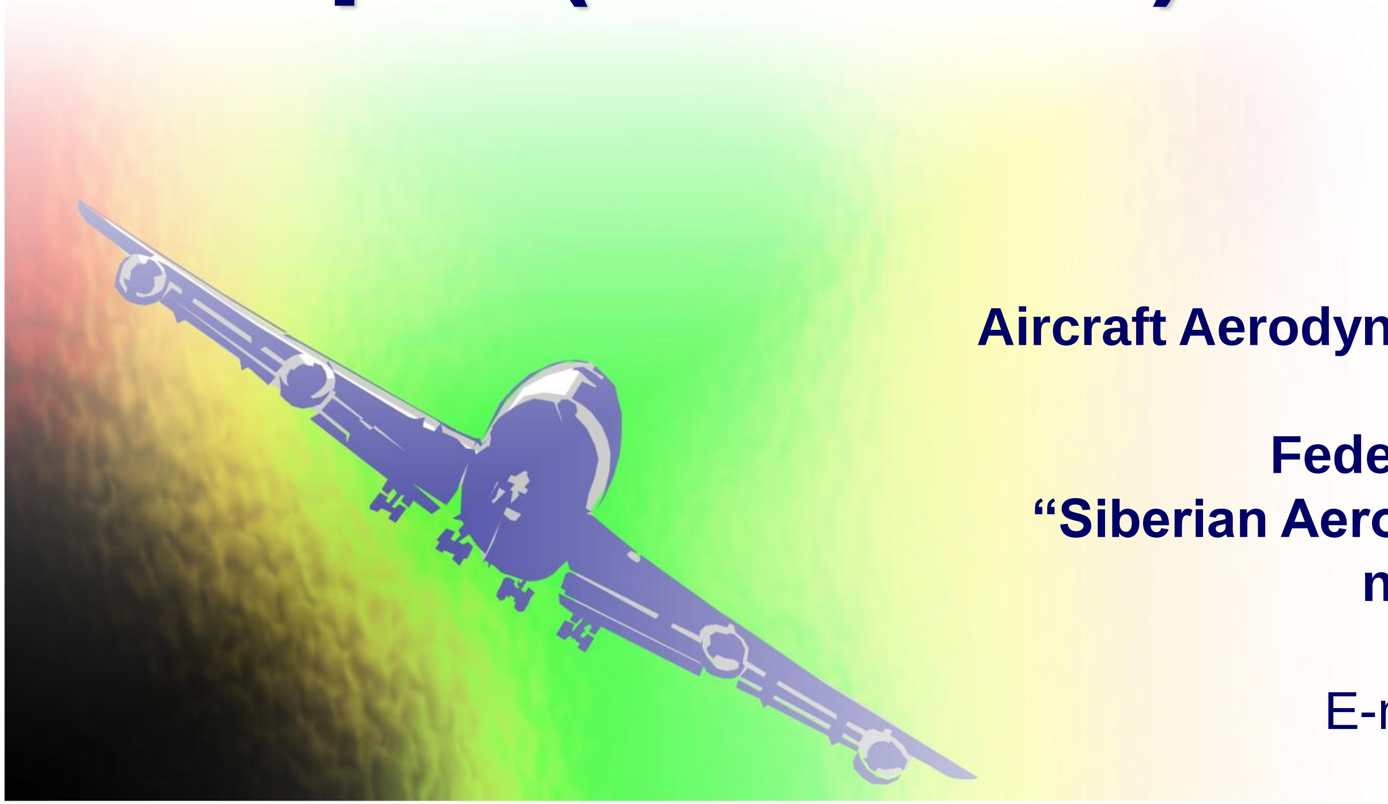

Dr. Ivan Y. Burdun
Lead Scientist
Aircraft Aerodynamics and Flight Dynamics
Research Division
Federal State Unitary Enterprise
“Siberian Aeronautical Research Institute
n.a. S.A.Chaplygin” (SibNIA)
Novosibirsk, Russia
E-mail: ivan.burdun@gmail.com

Research Formulation

Problem	Flight safety performance of an aircraft/project in complex (multi-factor) situations.
Solution Approach	‘Knowledge is Power’. Virtualization of future flight operation under complex conditions through system modeling and simulation. System model is knowledge generator of complex flight situation domains.
Goal	Develop and demonstrate a technique for predicting aircraft flight safety performance in complex situational domains.
Tasks	Theory advancement. Development of implementation technique. Design of flight M&S experiments. Running simulations. Documenting, processing and analysis of results. Development of recommendations on technique application in aircraft design and T&E.
Methods & Tools	Experimental and computational aerodynamics of aircraft, aircraft flight dynamics, situational control, numeric techniques, simulation experiment, artificial intelligence, graph theory, tree data structures, computer graphics, Fortran, VATES (v.7) proprietary software tool, PC Pentium-IV, MS Windows, MS Office, Pfe and MAGE freeware, etc.

Legend:

Classic techniques
Modern techniques

⇒ Classic techniques + modern techniques = new analytical potential.

Micro- and Macro-Structure Of Flight Situation Model

Micro-structure

Macro-structure

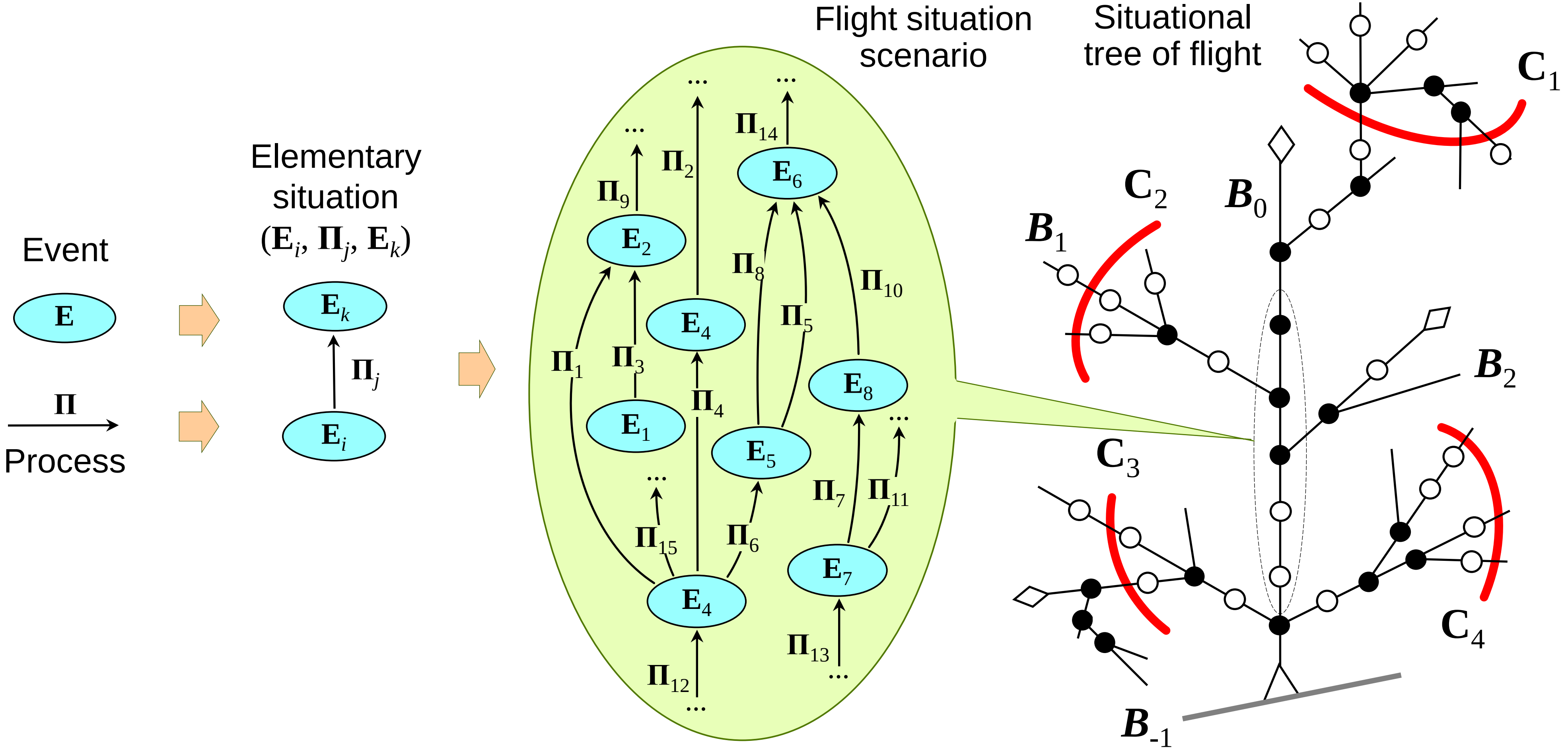

Legend: E$_i$ - flight event; Π$_j$ – flight process; C$_m$ – fuzzy constraint; ○ - system reference state; ● - system branching state (‘bud’); ◊ - system target state (‘leaf’); △ - system source state (‘root’); ***B***$_{-1}$ – parent branch; ***B***$_0$ – main branch or ‘trunk’ (baseline scenario); ***B***$_n$ – nth-order derivative branch (scenario with *n* operational factors involved, *n*=1, 2, …).

Flight Safety Performance Virtual T&E Cycle

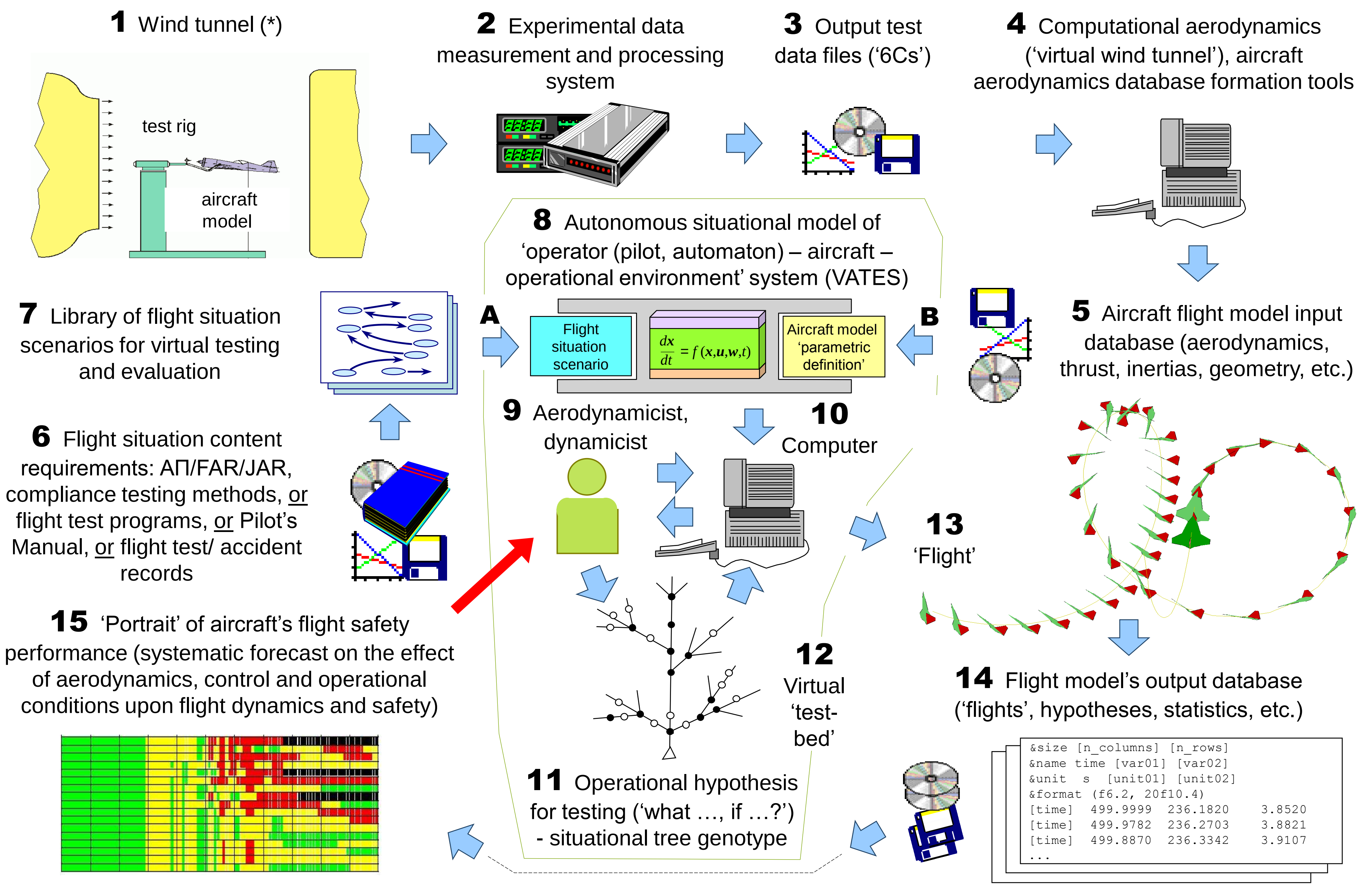

1 Wind tunnel (*)

2 Experimental data measurement and processing system

3 Output test data files ('6Cs')

4 Computational aerodynamics ('virtual wind tunnel'), aircraft aerodynamics database formation tools

5 Aircraft flight model input database (aerodynamics, thrust, inertias, geometry, etc.)

6 Flight situation content requirements: АП/FAR/JAR, compliance testing methods, <u>or</u> flight test programs, <u>or</u> Pilot's Manual, <u>or</u> flight test/ accident records

7 Library of flight situation scenarios for virtual testing and evaluation

8 Autonomous situational model of 'operator (pilot, automaton) – aircraft – operational environment' system (VATES)

9 Aerodynamicist, dynamicist

10 Computer

11 Operational hypothesis for testing ('what …, if …?') - situational tree genotype

12 Virtual 'test-bed'

13 'Flight'

14 Flight model's output database ('flights', hypotheses, statistics, etc.)

```
&size [n_columns] [n_rows]
&name time [var01] [var02]
&unit  s  [unit01] [unit02]
&format (f6.2, 20f10.4)
[time]  499.9999  236.1820    3.8520
[time]  499.9782  236.2703    3.8821
[time]  499.8870  236.3342    3.9107
...
```

15 'Portrait' of aircraft's flight safety performance (systematic forecast on the effect of aerodynamics, control and operational conditions upon flight dynamics and safety)

<u>Legend</u>: ⇨ - direction of information flow processing; **1**, …, **15** - flight safety T&E process components; (*) – courtesy of Dr. Nikolai Sohi;
➔ - feedback link; **A** and **B** – model's two main input data sets.

Flight Safety Palette. Fuzzy Constraint

Safety Colors

Flight Safety Palette →

- 🟩 - green (‘norm’), ξ_G
- 🟨 - yellow (‘attention’), ξ_A
- 🟥 - red (‘danger’), ξ_R
- ⬛ - black (‘catastrophe’), ξ_B
- ⬜ - grey/white (‘uncertainty’), ξ_W

⇒ Color is, perhaps, most natural and most effective medium for communicating safety-related information to/from a human expert or operator.

Fuzzy Constraint Example

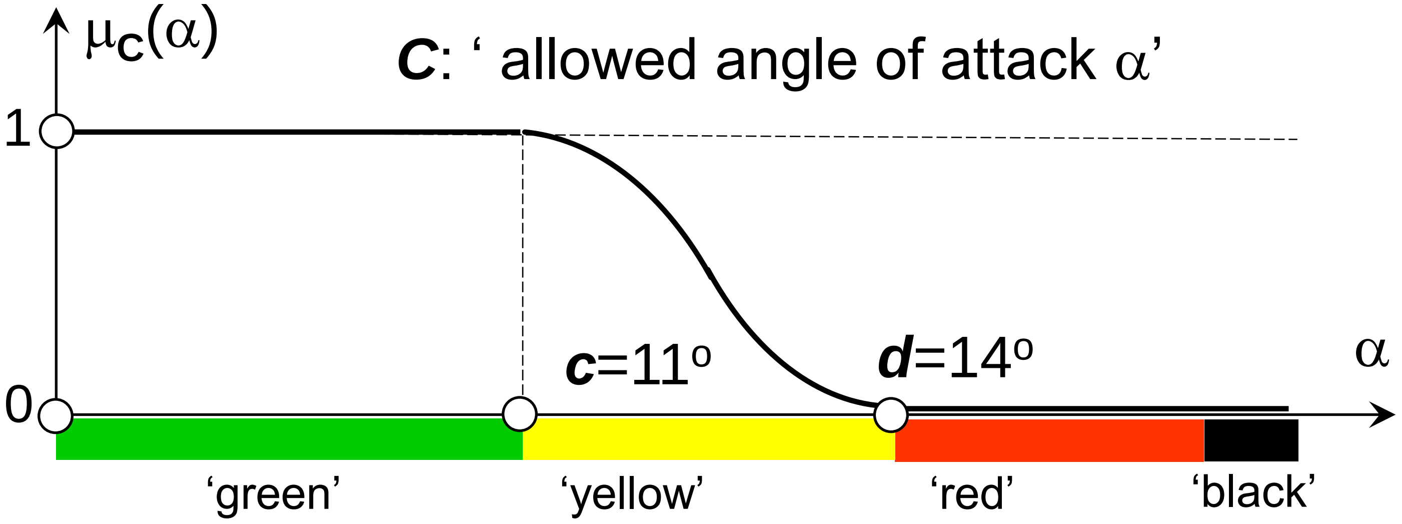

Legend: ***c***, ***d*** – characteristic points of fuzzy set-constraint ***C*** carrier, $\mu_C(x)$ – L.A. Zadeh membership function of fuzzy set.

⇒ Operational constraints, especially under complex flight conditions, are not known precisely; they are inherently ‘fuzzy’. The notion of fuzzy constraint by L.A. Zadeh is employed for approximate measurement of the current level (i.e. at time instant *t*) of aircraft flight safety. In overall, 20 constraints are defined and monitored in this study.

Partial and Integral Flight Safety Spectra

Integral Flight Safety Spectrum (IFSS) – Calculation Algorithm

$$(\forall t)(t\in[t_*;t^*])(\exists\xi(x_k(t))(\xi(x_k(t))\in\{\xi_W, \xi_G, \xi_A, \xi_R, \xi_B, \ldots\}$$

$$\wedge (\xi_W< \xi_G< \xi_A< \xi_R< \xi_B))(\xi(t) = max\ \xi(x_k(t)), k=1, \ldots, p)$$

$$\Rightarrow (\xi(t)\in\Sigma \wedge \Sigma = \xi(t_*) \| \xi(t_*+\Delta) \| \xi(t_*+2\Delta) \| \ldots \| \xi(t^*))$$

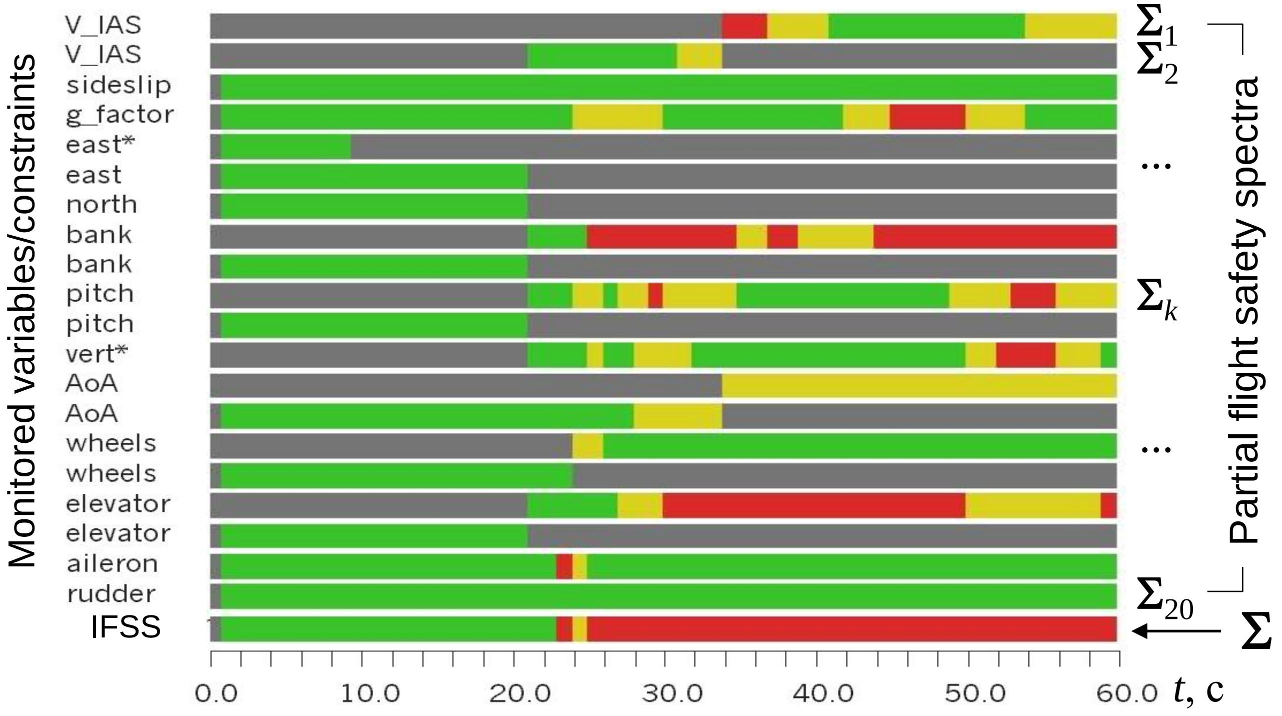

Flight Safety Palette

🟩 - green (‘norm’), ξ_G

🟨 - yellow (‘attention’), ξ_A

🟥 - red (‘danger’), ξ_R

⬛ - black (‘catastrophe’), ξ_B

⬜ - gray/white (‘uncertainty’), ξ_W

Legend: Σ_k – partial safety spectrum for variable x_k, $k=1, \ldots, p$; p – total number of monitored constraints/variables, $p=20$. Σ – integral safety spectrum; t – flight time; ξ_i – safety color from safety palette, $i\in\{$B (black), R (red), A (yellow), G (green),…$\}$; < – ‘colder than’ operation for comparing two safety colors; *max* – operation of selecting the ‘hottest’ color at time instant t; $\|$ - safety colors concatenation operation in Σ; $[t_*; t^*]$ – examined flight time interval; Δ – spectrum construction time increment.

$\Rightarrow$ After having measured current safety levels along time axis for all variables x_k of the flight situation under study, a family of partial flight safety spectra Σ_k, $k=1, \ldots, p$, and an integral flight safety spectrum Σ are obtained. Sources of flight situation data are: computer flight simulation, manned flight simulation, flight testing or flight operation.

Flight Safety Categories

Flight Safety Category			Flight Situation Classification Criterion
Color	Code	Name	
🟩	**I**	**Safe**	The system state resides mainly inside the 'green' zone. As a maximum, the system state may stay, for a *short time*, in close proximity to operational constraints, i.e. inside the ‘amber’ zone, but must leave it by the end of the flight situation
🟩	**II-a**	**Conditionally Safe – a**	As a maximum, the system state may stay for a *medium time* in close proximity to operational constraints, i.e. inside the ‘amber’ zone
🟨	**II-b**	**Conditionally Safe – b**	As a maximum, the system state may stay for a *long time* in close proximity to operational constraints, i.e. inside the ‘amber’ zone
🟧	**III**	**Potentially Unsafe**	As a maximum, the system state may violate operational constraints, i.e. enter the ‘red’ zone, for a *short or medium time*, but must leave it by the end of the situation
🟥	**IV**	**Dangerous (Prohibited)**	As a maximum, the system state may stay beyond operational constraints, i.e. inside the ‘red’ zone, for a *long time* or till the end of the flight situation
⬛	**V**	**Catastrophic (‘Chain Reaction’)**	There is at least one (for a *short time*) occurrence of a ‘black’ violation of any operational constraint

⇒ In order to measure safety performance of a flight situation in overall, a special ‘safety ruler’ consisting of five classification categories **I**, …, **V** is employed. Why five? – because experts cannot reliably recognize and use more than 5-10 gradations of a complex, difficult-to-formalize system-level property (e.g.: Cooper-Harper scale). ‘Light green’, RGB (192; 255; 0), and ‘orange’, RGB (255; 192; 0), are interim colors used to denote Categories **II-a** and **III**.

Flight Safety 'Topology'

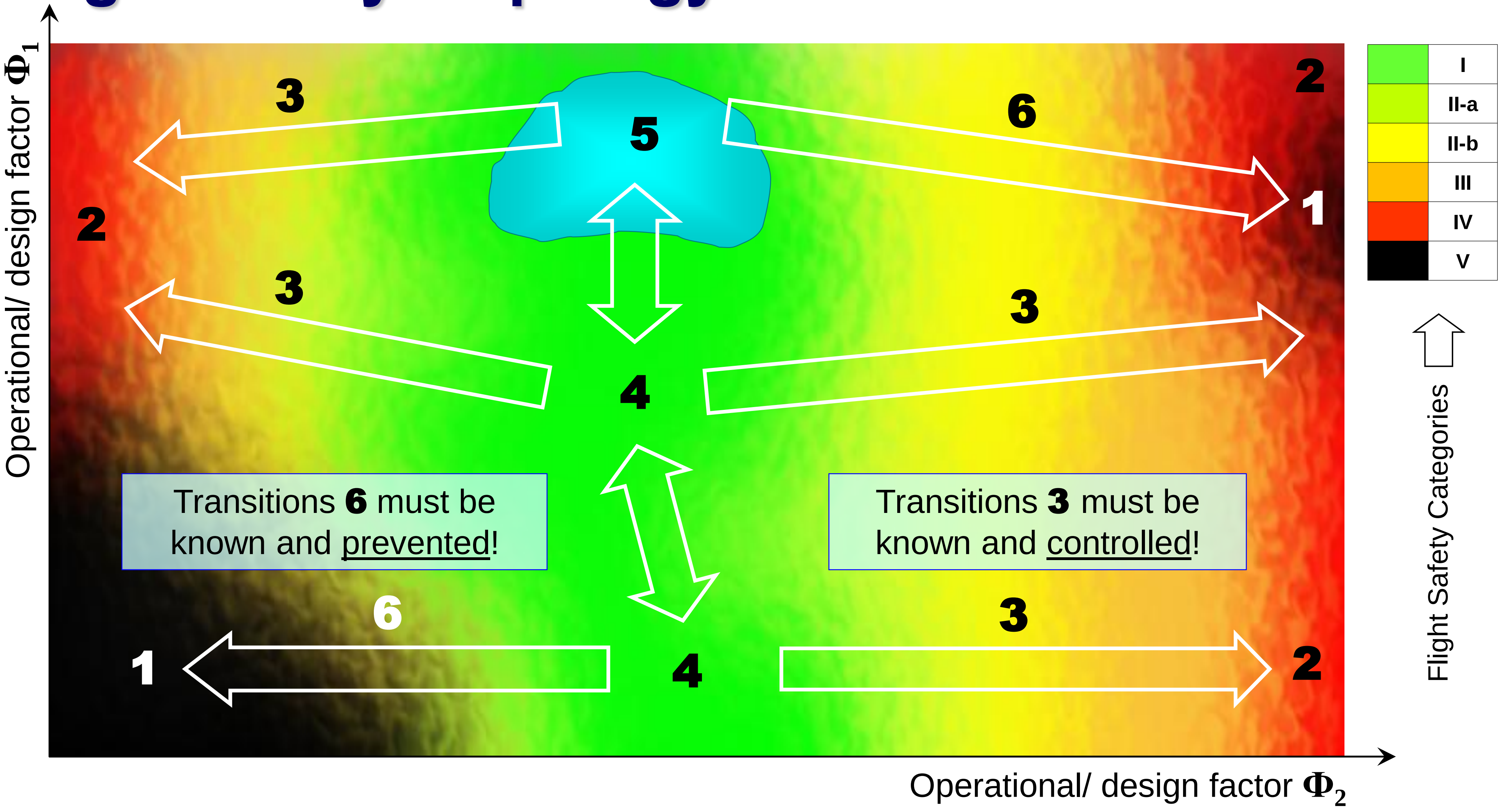

Transitions **6** must be known and <u>prevented</u>!

Transitions **3** must be known and <u>controlled</u>!

⇒ **1**, **2**,…, **6** - main object types of flight safety 'topology':

1 'Abyss' (catastrophe)

2 'Hill' (danger)

3 'Slope' (reversible state transitions)

4 'Valley' (standard safety, norm)

5 'Lake' (maximum safety, optimum)

6 'Precipice' (abrupt, irreversible state transitions,'chain reaction')

Baseline Flight Scenarios

$\mathbf{S}_i$	Content description
$\mathbf{S}_1$	Normal takeoff, maintaining commanded flight path and bank angles during initial climb
$\mathbf{S}_2$	Normal takeoff under crosswind and given runway's surface conditions, maintaining commanded flight path and bank angles during initial climb
$\mathbf{S}_3$	Continued takeoff (left-hand engine out at given V_{EF}), maintaining commanded flight path and bank angles during initial climb
$\mathbf{S}_4$	Normal takeoff under wind shear conditions, maintaining commanded flight path and bank angles during initial climb
$\mathbf{S}_5$	Continued takeoff (left-hand engine out at given V_{EF}), under crosswind conditions, maintaining commanded flight path and bank angles during initial climb

$\Rightarrow$ Baseline scenario $\mathbf{S}_i$ is a plan of some 'central' (any standard or non-standard) flight situation, which variations (derivative cases) are virtually tested in autonomous M&S experiments. The goal is to evaluate effects of selected key operational (and/or design) factors/hypotheses on flight safety. The sources of data for baseline scenarios are: airworthiness requirements (АП, FAR, JAR), flight test data/programs, ACs, Pilot's Manuals, real flight data records, flight accidents/incidents statistics.

Joint Graph of Baseline Scenarios

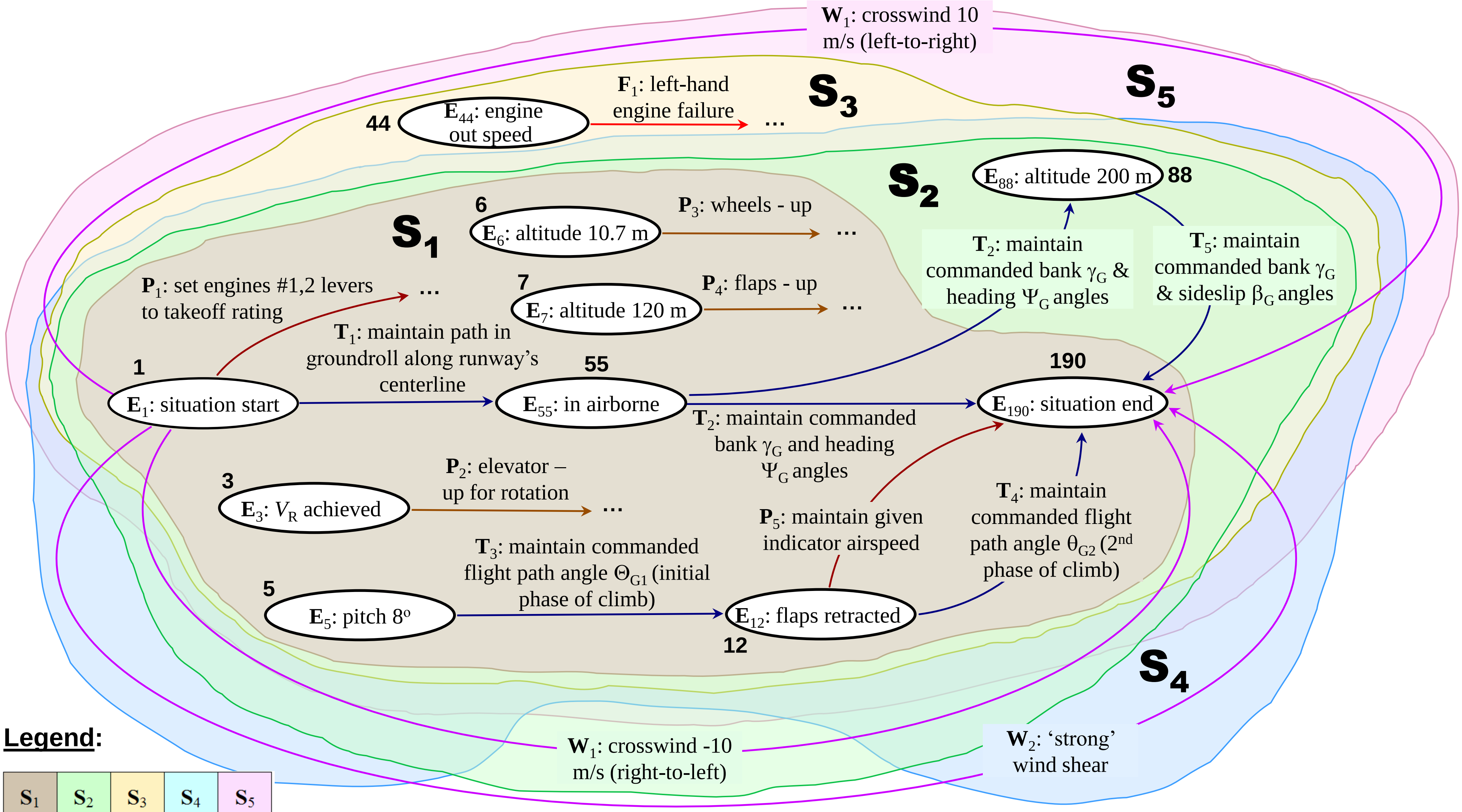

Legend:

S_1	S_2	S_3	S_4	S_5

44 E_{44}: engine out speed - event

F_1: left-hand engine failure → - process

⇒ Scenario is depicted as a directed graph. It defines logic and content of a flight situation. It is also clear to the pilot. Scenarios $\mathbf{S}_1$, …, $\mathbf{S}_5$ are structurally close. They can be easily modified.

Operational Factors Selected for Testing

Φ_i	Definition	x_j
Φ_1	Longitudinal C.G. location	$\overline{x}_{CG}$
Φ_2	Rotation airspeed	V_{R}
Φ_3	Elevator deflection for rotation	$\Delta\delta_{\mathrm{e}}$
Φ_4	Wheels – runway surface adhesion factor	μ
Φ_5	Cross wind velocity	W_{yg}
Φ_6	‘Flaps-up’ start altitude	H_{FL}
Φ_7	Commanded flight path angle during initial phase of climb	θ_{G1}
Φ_8	Commanded flight path angle during 2nd phase of climb	θ_{G2}
Φ_9	Intensity of wind shear	k_{W}
Φ_{10}	Engines power rating at takeoff	k_{P}
Φ_{11}	Commanded bank angle	γ_{G}
Φ_{12}	‘Engine out’ airspeed	V_{EF}
Φ_{13}	Left-hand engine failure at V_{EF}	ζ_{LHE}

⇒ Operational /design factors are modified or new events and/or processes, which - after having been added to a baseline scenario - can improve (or worsen) the aircraft safety performance. There are three groups of operational factors: ‘operator’, ‘aircraft’ and ‘external environment’. The sources of information on operational factors are national airworthiness requirements, FMEA, statistics on flight operations, accidents/incidents.

Design Field of Operational Hypotheses

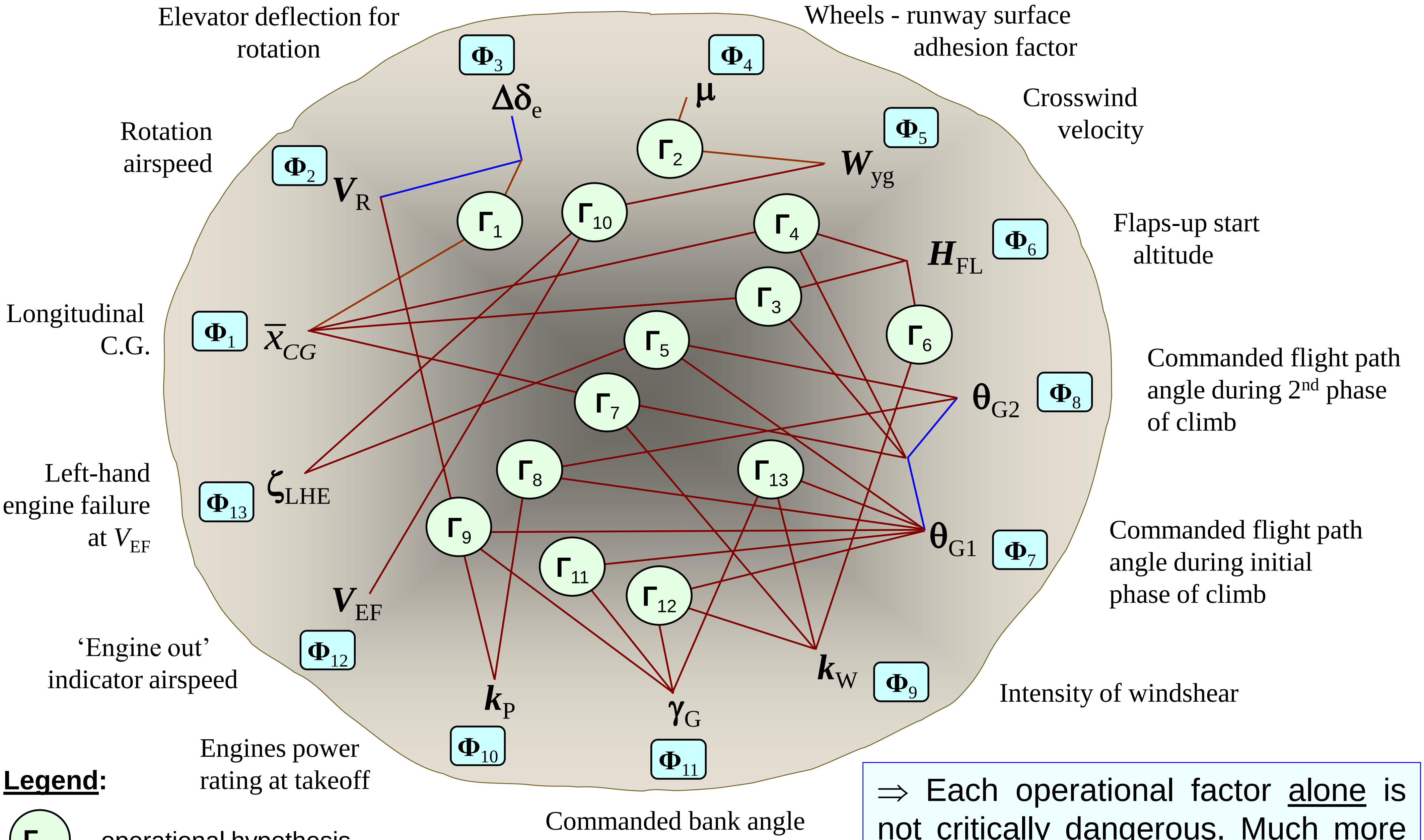

Legend:

Γ13 - operational hypothesis

W_{yg} Φ5 Cross wind velocity - operational factor

independent / dependent - link between factors in Γ

⇒ Each operational factor alone is not critically dangerous. Much more important to learn in advance effects of their combinations on flight safety.

Plan & Statistics of Simulation Experiments

$\mathbf{S}_i$	Operational Hypothesis			n	$i_1, \ldots, i_n$	Δt, s	$\Im\vert\, \mathbf{S}_i\cdot\mathbf{\Gamma}_k$, hrs
	$\mathbf{\Gamma}_k$	'Formula'	$N(\mathbf{\Phi})$				
$\mathbf{S}_1$	$\mathbf{\Gamma}_1$	$\bar{x}_{CG}\times(V_{\mathrm{R}}+\Delta\delta_{\mathrm{e}})$	3	66	101, …, 166	90	1.65
$\mathbf{S}_2$	$\mathbf{\Gamma}_2$	$W_{\mathrm{yg}}\times\mu$	2	63	201, …, 263	60	1.05
$\mathbf{S}_1$	$\mathbf{\Gamma}_3$	$\bar{x}_{CG}\times(\theta_{\mathrm{G1}}+\theta_{\mathrm{G2}})\times H_{\mathrm{FL}}\ (\bar{x}_{CG}=\bar{x}_{CG\min})$	4	35	301, …, 335	90	0.875
$\mathbf{S}_1$	$\mathbf{\Gamma}_4$	$\bar{x}_{CG}\times(\theta_{\mathrm{G1}}+\theta_{\mathrm{G2}})\times H_{\mathrm{FL}}\ (\bar{x}_{CG}=\bar{x}_{CG\max})$	4	35	401, …, 435	90	0.875
$\mathbf{S}_3$	$\mathbf{\Gamma}_5$	$\zeta_{\mathrm{LHE}}\times\theta_{\mathrm{G1}}\times\theta_{\mathrm{G2}}\ (V_{\mathrm{EF}}=150$ км/ч$)$	3	42	501, …, 542	90	1.05
$\mathbf{S}_4$	$\mathbf{\Gamma}_6$	$k_{\mathrm{W}}\times H_{\mathrm{FL}}$	2	78	601, …, 678	100	2.167
$\mathbf{S}_4$	$\mathbf{\Gamma}_7$	$\bar{x}_{CG}\times k_{\mathrm{W}}\times(\theta_{\mathrm{G1}}+\theta_{\mathrm{G2}})\ (\bar{x}_{CG}=\bar{x}_{CG\min})$	4	78	701, …, 778	100	2.167
$\mathbf{S}_1$	$\mathbf{\Gamma}_8$	$k_{\mathrm{P}}\times\theta_{\mathrm{G1}}\times\theta_{\mathrm{G2}}$	3	126	801, …, 926	90	3.15
$\mathbf{S}_1$	$\mathbf{\Gamma}_9$	$V_{\mathrm{R}}\times k_{\mathrm{P}}\times\theta_{\mathrm{G1}}\times\gamma_{\mathrm{G}}$	4	150	1901, …, 2050	60	2.5
$\mathbf{S}_5$	$\mathbf{\Gamma}_{10}$	$\zeta_{\mathrm{LHE}}\times V_{\mathrm{EF}}\times W_{\mathrm{yg}}$	3	104	1001, …, 1104	120	3.467
$\mathbf{S}_1$	$\mathbf{\Gamma}_{11}$	$\theta_{\mathrm{G1}}\times\gamma_{\mathrm{G}}$	2	130	2101, …, 2230	60	2.167
$\mathbf{S}_4$	$\mathbf{\Gamma}_{12}$	$k_{\mathrm{W}}\times\theta_{\mathrm{G1}}\times\gamma_{\mathrm{G}}\ (k_{\mathrm{W}}=1)$	3	130	1201, …, 1330	60	2.167
$\mathbf{S}_4$	$\mathbf{\Gamma}_{13}$	$k_{\mathrm{W}}\times\theta_{\mathrm{G1}}\times\gamma_{\mathrm{G}}\ (k_{\mathrm{W}}=1.5)$	3	130	3201, …, 3330	60	2.167
Total virtual flight test experience accumulated in 'forest' $\{\mathbf{S}_1\cdot\mathbf{\Gamma}_1, \ldots, \mathbf{S}_4\cdot\mathbf{\Gamma}_{13}\}$, hrs:							**~24.6**

Legend: i – code of baseline scenario $\mathbf{S}_i$, i=1, …, 5; k – code of operational hypothesis $\mathbf{\Gamma}_k$, k=1, …, 13; $N(\mathbf{\Phi})$ – number of operational factors in $\mathbf{\Gamma}_k$; n – size of 'flight' series $\Omega_k(\boldsymbol{F})$, $\Omega_k(\boldsymbol{F})=\{\boldsymbol{F}_{i_1}, \ldots, \boldsymbol{F}_j, \ldots, \boldsymbol{F}_{i_n}\}$, $n=i_n-i_1+1$, j – 'flight' code; Δt – planned duration of 'flight' $\boldsymbol{F}_j$, $\boldsymbol{F}_j\in\Omega_k(\boldsymbol{F})$; $\Im\vert\mathbf{S}_i\cdot\mathbf{\Gamma}_k$ – 'virtual flight test experience' accumulated in tree $\mathbf{S}_i\cdot\mathbf{\Gamma}_k$; notation of coordinate axes corresponds to ISO 1151.

⇒ Composition of baseline scenario $\mathbf{S}_i$ and operational hypothesis $\mathbf{\Gamma}_k$ results in a family of derivative ('neighboring') situations – a 'situational tree' $\mathbf{S}_i\cdot\mathbf{\Gamma}_k$. Construction of a 'forest' of such trees - based on FMEA, flight test/operation/ incidents/accidents data - and studying their safety 'topology' is the goal of virtual flight T&E.

Situational Tree - $S_1 \cdot \Gamma_{11}$ Composition Example

Normal Takeoff. Variations/ Errors Of Selection Of Commanded Flight Path And Bank Angles During Initial Climb

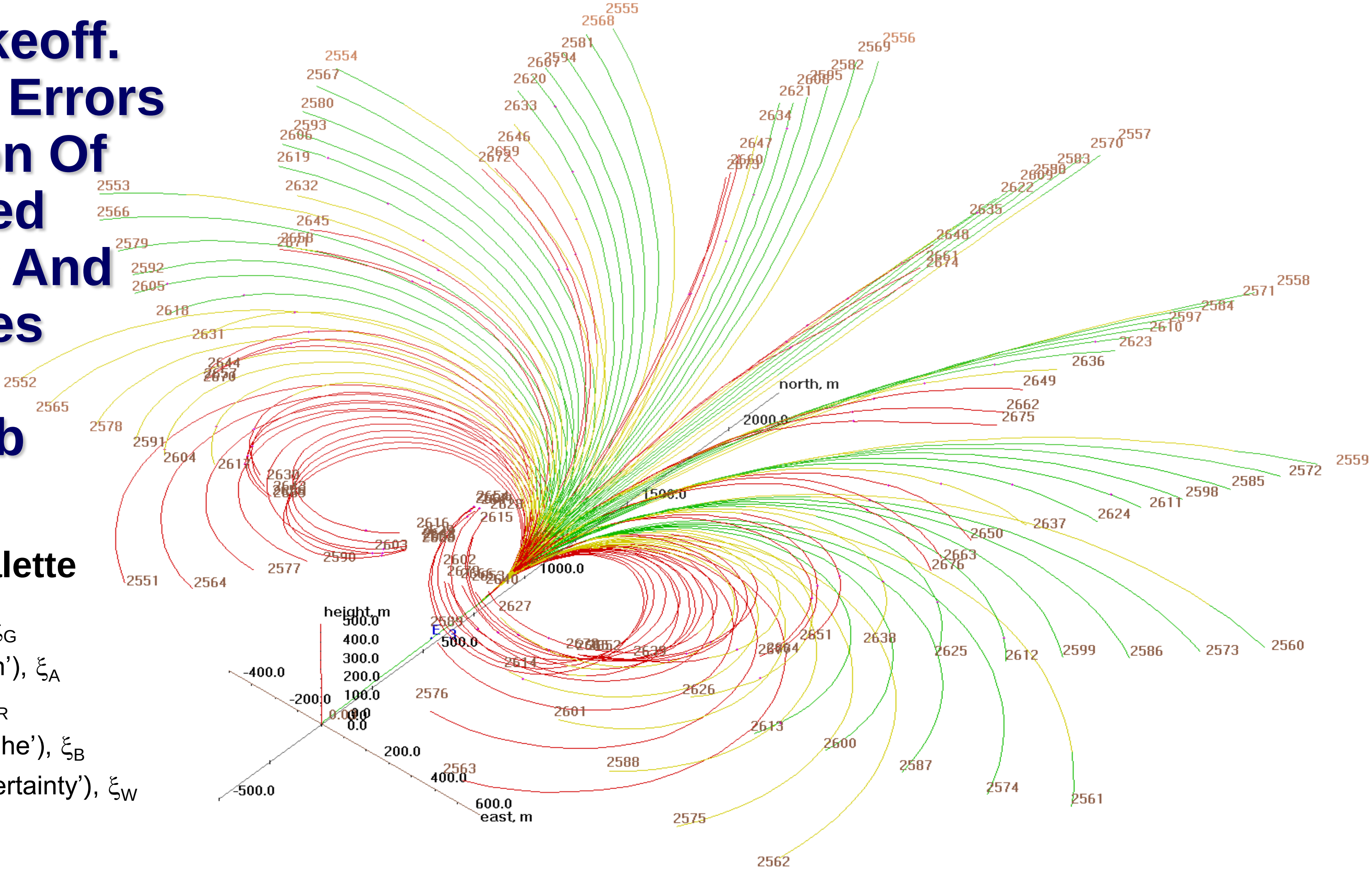

Flight Safety Palette

- 🟩 - green ('norm'), ξ_G
- 🟨 - yellow ('attention'), ξ_A
- 🟥 - red ('danger'), ξ_R
- ⬛ - black ('catastrophe'), ξ_B
- ⬜ - gray/white ('uncertainty'), ξ_W

Legend: $\boldsymbol{T}_{130}=\{\boldsymbol{F}_{2101}, \ldots, \boldsymbol{F}_{2230}\}$ – situational tree, $\boldsymbol{F}_k$ – 'flight'; $\mathbf{B}_i$ - branch, $\mathbf{B}_i \equiv \boldsymbol{F}_k$, k=2551/2101, …, 2680/2230, i=1, …, $N(\boldsymbol{T}_{130})$, $N(\boldsymbol{T}_{130})$=130 – number of branches in $\boldsymbol{T}_{130}$; $\boldsymbol{\Gamma}(\boldsymbol{\Phi}_7 \times \boldsymbol{\Phi}_{211})$ – operational hypothesis implemented in $\boldsymbol{T}_{130}$, $\boldsymbol{\Gamma}(\boldsymbol{\Phi}_7 \times \boldsymbol{\Phi}_{11}) = \Omega(\boldsymbol{\Phi}_7) \times \Omega(\boldsymbol{\Phi}_{11})$; $\boldsymbol{\Phi}_7$ – operational factor 'commanded flight path angle', $\boldsymbol{\Phi}_7 \equiv \theta_{G1}$, $\Omega(\boldsymbol{\Phi}_7)=\{2^o, 4^o, \ldots, 20^o\}$; $\boldsymbol{\Phi}_{11}$ – operational factor 'commanded bank angle', $\boldsymbol{\Phi}_{11} \equiv \gamma_{G1}$, $\Omega(\boldsymbol{\Phi}_{11})=\{-45^o, -37.5^o, \ldots, +45^o\}$; $\Delta t(\mathbf{B}_i)$ – branch length measured in time units t, $(\forall i)(i=1, \ldots, N(\boldsymbol{T}_{130}))(\Delta t(\mathbf{B}_i)=60$ s); (north, east, height) ≡ (N, E, H) – $\boldsymbol{T}_{130}$ diagram axes.

Composition $S_1 \cdot \Gamma_1$

Normal Takeoff. Variations Of C.G. Location And V_R Speed (With Correction Of Elevator Deflection In Rotation)

Integral Flight Safety Spectra (IFSS)

Flight situation code

Tested operational factors

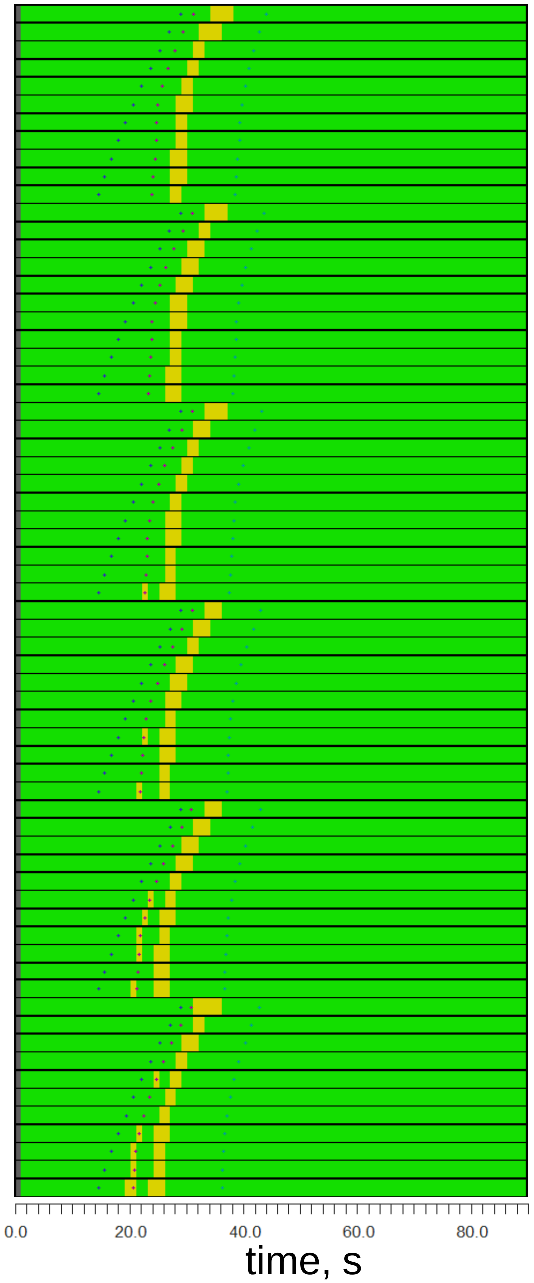

#	m_P	m_F	V_R	$\Delta\delta_e$
166	2400.00	400.00	250.00	-5.00
165	2400.00	400.00	240.00	-6.00
164	2400.00	400.00	230.00	-7.00
163	2400.00	400.00	220.00	-8.00
162	2400.00	400.00	210.00	-9.00
161	2400.00	400.00	200.00	-10.00
160	2400.00	400.00	190.00	-11.00
159	2400.00	400.00	180.00	-12.00
158	2400.00	400.00	170.00	-13.00
157	2400.00	400.00	160.00	-14.00
156	2400.00	400.00	150.00	-15.00
155	2000.00	800.00	250.00	-5.00
154	2000.00	800.00	240.00	-6.00
153	2000.00	800.00	230.00	-7.00
152	2000.00	800.00	220.00	-8.00
151	2000.00	800.00	210.00	-9.00
150	2000.00	800.00	200.00	-10.00
149	2000.00	800.00	190.00	-11.00
148	2000.00	800.00	180.00	-12.00
147	2000.00	800.00	170.00	-13.00
146	2000.00	800.00	160.00	-14.00
145	2000.00	800.00	150.00	-15.00
144	1600.00	1200.00	250.00	-5.00
143	1600.00	1200.00	240.00	-6.00
142	1600.00	1200.00	230.00	-7.00
141	1600.00	1200.00	220.00	-8.00
140	1600.00	1200.00	210.00	-9.00
139	1600.00	1200.00	200.00	-10.00
138	1600.00	1200.00	190.00	-11.00
137	1600.00	1200.00	180.00	-12.00
136	1600.00	1200.00	170.00	-13.00
135	1600.00	1200.00	160.00	-14.00
134	1600.00	1200.00	150.00	-15.00
133	1200.00	1600.00	250.00	-5.00
132	1200.00	1600.00	240.00	-6.00
131	1200.00	1600.00	230.00	-7.00
130	1200.00	1600.00	220.00	-8.00
129	1200.00	1600.00	210.00	-9.00
128	1200.00	1600.00	200.00	-10.00
127	1200.00	1600.00	190.00	-11.00
126	1200.00	1600.00	180.00	-12.00
125	1200.00	1600.00	170.00	-13.00
124	1200.00	1600.00	160.00	-14.00
123	1200.00	1600.00	150.00	-15.00
122	800.00	2000.00	250.00	-5.00
121	800.00	2000.00	240.00	-6.00
120	800.00	2000.00	230.00	-7.00
119	800.00	2000.00	220.00	-8.00
118	800.00	2000.00	210.00	-9.00
117	800.00	2000.00	200.00	-10.00
116	800.00	2000.00	190.00	-11.00
115	800.00	2000.00	180.00	-12.00
114	800.00	2000.00	170.00	-13.00
113	800.00	2000.00	160.00	-14.00
112	800.00	2000.00	150.00	-15.00
111	400.00	2400.00	250.00	-5.00
110	400.00	2400.00	240.00	-6.00
109	400.00	2400.00	230.00	-7.00
108	400.00	2400.00	220.00	-8.00
107	400.00	2400.00	210.00	-9.00
106	400.00	2400.00	200.00	-10.00
105	400.00	2400.00	190.00	-11.00
104	400.00	2400.00	180.00	-12.00
103	400.00	2400.00	170.00	-13.00
102	400.00	2400.00	160.00	-14.00
101	400.00	2400.00	150.00	-15.00

Category	ξ^j	χ^j, %
I	🟩	100
II-a	🟩	0
II-b	🟨	0
III	🟧	0
IV	🟥	0
V	⬛	0
‘Flights’ in total - 66		100

Safety Chances Pie Chart

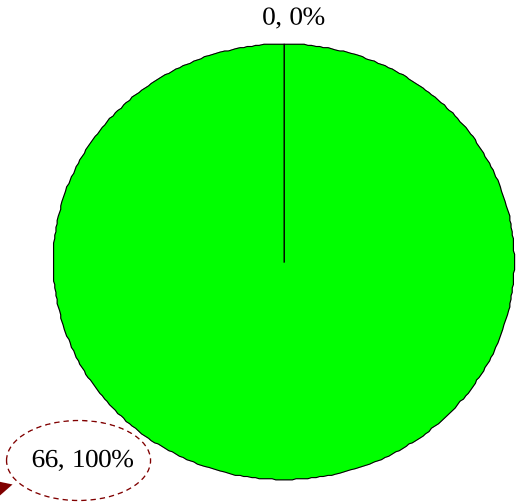

Legend: in n^j, χ^j% n^j – number of ‘flights’ belonging to Cat. ξ^j, χ^j% - percentage of ‘flights’ of Cat. ξ^j, j=**I**, …, **V**.

⇒ All situations from Composition $\mathbf{S}_1 \cdot \mathbf{\Gamma}_1$ are therefore safe, i.e. they belong to Category **I** cluster. Note how location of events $\mathbf{E}_3$ and $\mathbf{E}_7$ on IFSS is changed due to situation (operational factors).

$S_1 \cdot \Gamma_1$ Normal Takeoff. Variations Of C.G. Location And V_R Speed (With Correction Of Elevator Deflection In Rotation)

S_1: Normal takeoff, steering commanded flight path and bank angles during initial climb

$$\Gamma_1 = \Phi_1 \times (\Phi_2 + \Phi_3) \equiv \bar{x}_{CG} \times (V_R + \Delta\delta_e)$$

⇒ In FSW below, cell **1** located at ‘column **2** - row **3**’ crossing is a color code of flight safety Category of one situation from Composition **$S_1 \cdot \Gamma_1$**. This situation is obtained by combining values **4** and **5** of operational factors **6** and **7** in scenario **S_1**.

Flight Safety Window (FSW)

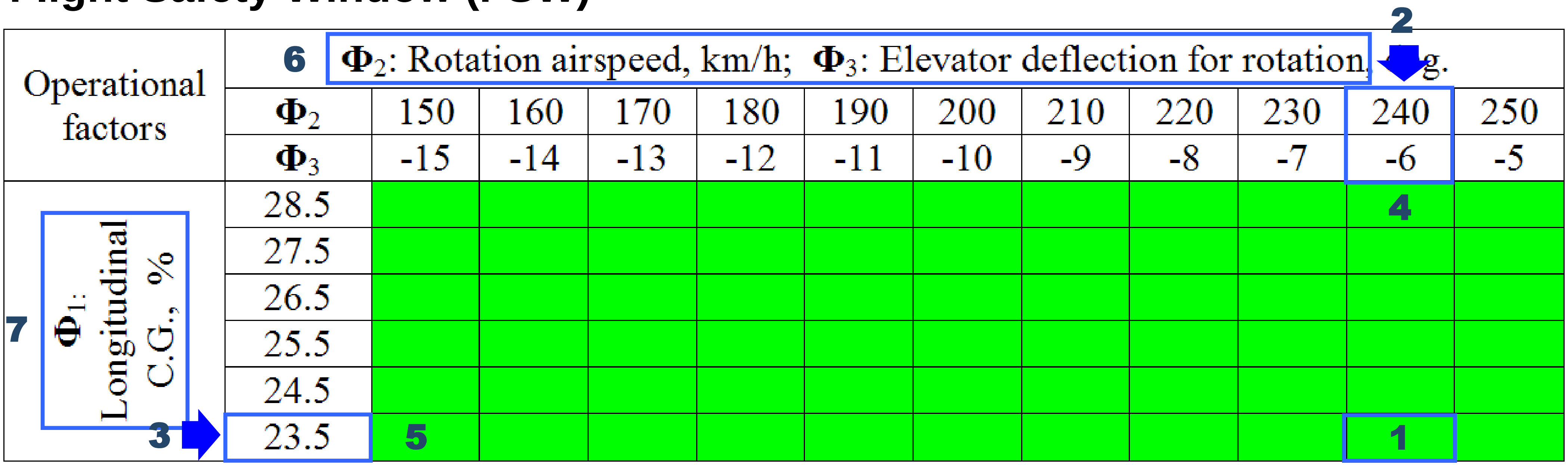

Operational factors	**6**	Φ_2: Rotation airspeed, km/h; Φ_3: Elevator deflection for rotation, deg.									**2**	
	Φ_2	150	160	170	180	190	200	210	220	230	240	250
	Φ_3	-15	-14	-13	-12	-11	-10	-9	-8	-7	-6	-5
7 $\Phi_{1:}$ Longitudinal C.G., %	28.5	🟩	🟩	🟩	🟩	🟩	🟩	🟩	🟩	🟩	🟩 **4**	🟩
	27.5	🟩	🟩	🟩	🟩	🟩	🟩	🟩	🟩	🟩	🟩	🟩
	26.5	🟩	🟩	🟩	🟩	🟩	🟩	🟩	🟩	🟩	🟩	🟩
	25.5	🟩	🟩	🟩	🟩	🟩	🟩	🟩	🟩	🟩	🟩	🟩
	24.5	🟩	🟩	🟩	🟩	🟩	🟩	🟩	🟩	🟩	🟩	🟩
3	23.5	🟩 **5**	🟩	🟩	🟩	🟩	🟩	🟩	🟩	🟩	🟩 **1**	🟩

⇒ This Flight Safety Window constructed for Composition **$S_1 \cdot \Gamma_1$** situations has ‘trivial topology’ – one continuous green ‘valley’. That is, for given aircraft/project all examined combinations of longitudinal C.G. location and V_R speed variations are acceptable by flight safety criteria (NB: provided that all other conditions of scenario **S_1** are fulfilled).

$S_2 \cdot \Gamma_2$ Normal Takeoff. Variations Of Crosswind Velocity And 'Wheels - Runway Surface' Adhesion Factor

IFSS

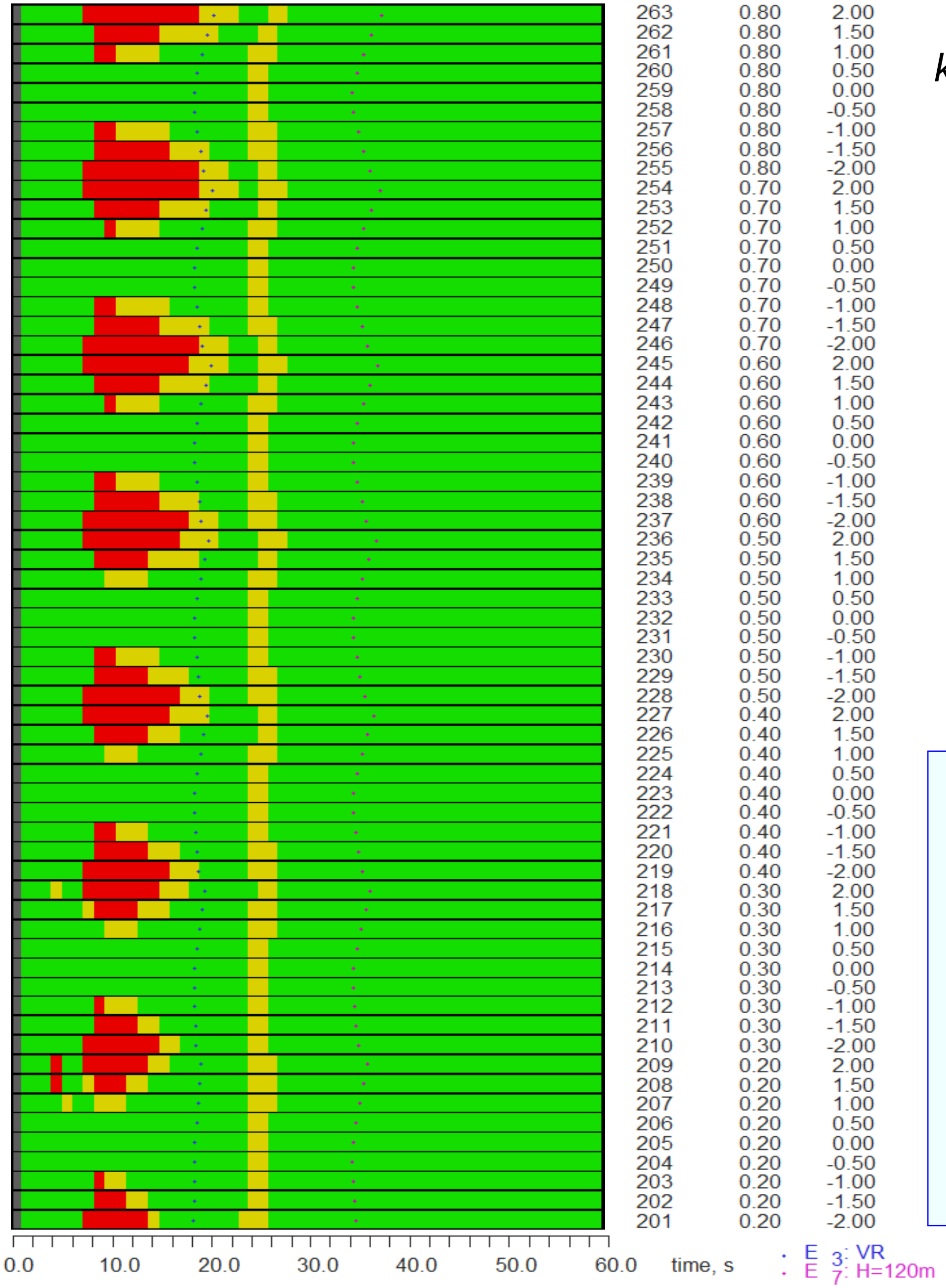

#	μ	$k \cdot W_{yg}$
263	0.80	2.00
262	0.80	1.50
261	0.80	1.00
260	0.80	0.50
259	0.80	0.00
258	0.80	-0.50
257	0.80	-1.00
256	0.80	-1.50
255	0.80	-2.00
254	0.70	2.00
253	0.70	1.50
252	0.70	1.00
251	0.70	0.50
250	0.70	0.00
249	0.70	-0.50
248	0.70	-1.00
247	0.70	-1.50
246	0.70	-2.00
245	0.60	2.00
244	0.60	1.50
243	0.60	1.00
242	0.60	0.50
241	0.60	0.00
240	0.60	-0.50
239	0.60	-1.00
238	0.60	-1.50
237	0.60	-2.00
236	0.50	2.00
235	0.50	1.50
234	0.50	1.00
233	0.50	0.50
232	0.50	0.00
231	0.50	-0.50
230	0.50	-1.00
229	0.50	-1.50
228	0.50	-2.00
227	0.40	2.00
226	0.40	1.50
225	0.40	1.00
224	0.40	0.50
223	0.40	0.00
222	0.40	-0.50
221	0.40	-1.00
220	0.40	-1.50
219	0.40	-2.00
218	0.30	2.00
217	0.30	1.50
216	0.30	1.00
215	0.30	0.50
214	0.30	0.00
213	0.30	-0.50
212	0.30	-1.00
211	0.30	-1.50
210	0.30	-2.00
209	0.20	2.00
208	0.20	1.50
207	0.20	1.00
206	0.20	0.50
205	0.20	0.00
204	0.20	-0.50
203	0.20	-1.00
202	0.20	-1.50
201	0.20	-2.00

$k=10^{-1}$

Safety Chances Pie Chart

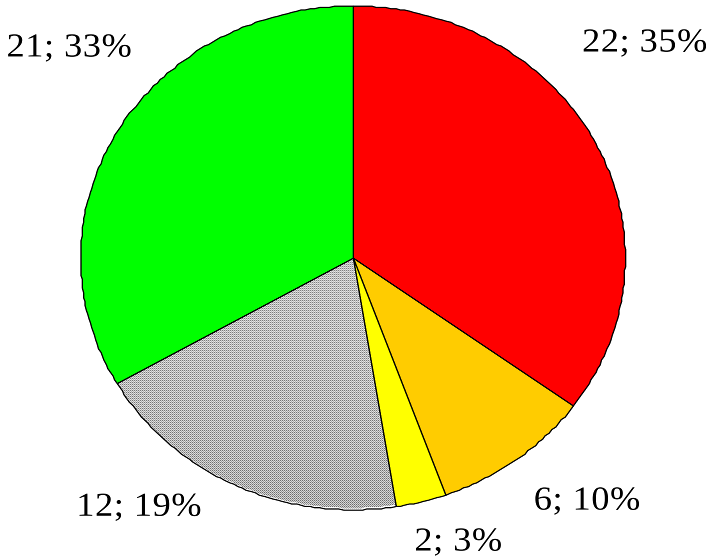

⇒ Variants with strong crosswind of |15|…|20| m/s exhibit danger during groundroll up to event $\mathbf{E}_3$ (V_R) - ref. next slide for FSW. These variants constitute 45% of all tested flight situations from composition $\mathbf{S}_2 \cdot \mathbf{\Gamma}_2$. Remaining situations (55%) are safe - they belong to Categories **I** and **II**. Note how the location of events $\mathbf{E}_3$ and $\mathbf{E}_7$ in IFSS is changed due to the effect of (μ, W_{yg}) combinations.

$S_2 \cdot \Gamma_2$ Normal Takeoff. Variations Of Crosswind Velocity And ‘Wheels – Runway Surface’ Adhesion Factor

$\mathbf{S}_2$: Normal takeoff under cross-wind and specified conditions of runway surface, steering commanded flight path and bank angles during initial climb

$$\mathbf{\Gamma}_2 = \mathbf{\Phi}_5 \times \mathbf{\Phi}_4 \equiv W_{yg} \times \mu$$

FSW

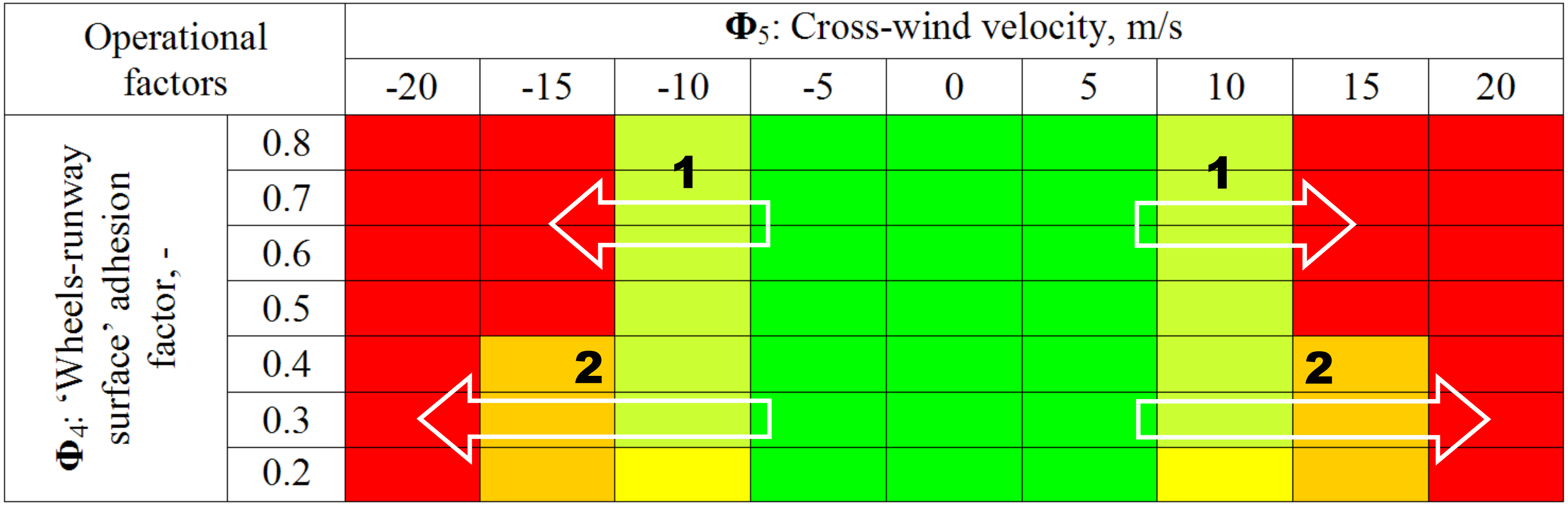

Operational factors		$\mathbf{\Phi}_5$: Cross-wind velocity, m/s								
		-20	-15	-10	-5	0	5	10	15	20
$\mathbf{\Phi}_4$: ‘Wheels-runway surface’ adhesion factor, -	0.8	🟥	🟥	🟨	🟩	🟩	🟩	🟨	🟥	🟥
	0.7	🟥	🟥	🟨	🟩	🟩	🟩	🟨	🟥	🟥
	0.6	🟥	🟥	🟨	🟩	🟩	🟩	🟨	🟥	🟥
	0.5	🟥	🟥	🟨	🟩	🟩	🟩	🟨	🟥	🟥
	0.4	🟥	🟧	🟨	🟩	🟩	🟩	🟨	🟧	🟥
	0.3	🟥	🟧	🟨	🟩	🟩	🟩	🟨	🟧	🟥
	0.2	🟥	🟧	🟡	🟩	🟩	🟩	🟡	🟧	🟥

⇒ Shown above is Flight Safety Window constructed for situational tree $\mathbf{S}_2 \cdot \mathbf{\Gamma}_2$. It contains one central green ‘valley’, two side red ‘hills’ and two connecting ‘slopes’: (**1**) a steep ‘slope’ – for dry and semi-wet runway, and (**2**) not steep ‘slope’ - for wet and water-covered runway. As the absolute value of cross-wind velocity increases, transitions from safe to dangerous states occur (1) sharply and (2) gradually, respectively. The shape and position of ‘crosswind velocity – adhesion factor’ constraints can be seen as well.

$S_1 \cdot \Gamma_3$ Normal Takeoff. Forward C.G. Location. Variations/ Errors Of Selection Of Commanded Flight Path Angles (Initial And 2nd Phases Of Climb) And Flaps-up Start Altitude

IFSS

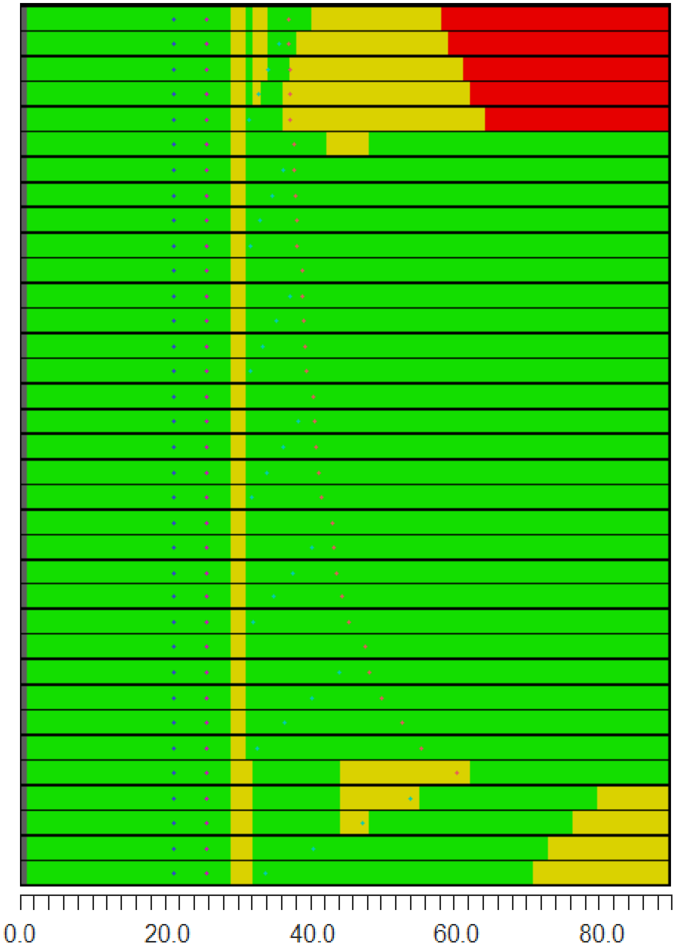

#	θ_{G1}	θ_{G2}	H_{FL}
335	14.00	12.00	120.00
334	14.00	12.00	100.00
333	14.00	12.00	80.00
332	14.00	12.00	60.00
331	14.00	12.00	40.00
330	12.00	10.00	120.00
329	12.00	10.00	100.00
328	12.00	10.00	80.00
327	12.00	10.00	60.00
326	12.00	10.00	40.00
325	10.00	8.00	120.00
324	10.00	8.00	100.00
323	10.00	8.00	80.00
322	10.00	8.00	60.00
321	10.00	8.00	40.00
320	8.00	6.00	120.00
319	8.00	6.00	100.00
318	8.00	6.00	80.00
317	8.00	6.00	60.00
316	8.00	6.00	40.00
315	6.00	4.00	120.00
314	6.00	4.00	100.00
313	6.00	4.00	80.00
312	6.00	4.00	60.00
311	6.00	4.00	40.00
310	4.00	2.00	120.00
309	4.00	2.00	100.00
308	4.00	2.00	80.00
307	4.00	2.00	60.00
306	4.00	2.00	40.00
305	2.00	0.00	120.00
304	2.00	0.00	100.00
303	2.00	0.00	80.00
302	2.00	0.00	60.00
301	2.00	0.00	40.00

Safety Chances Pie Chart

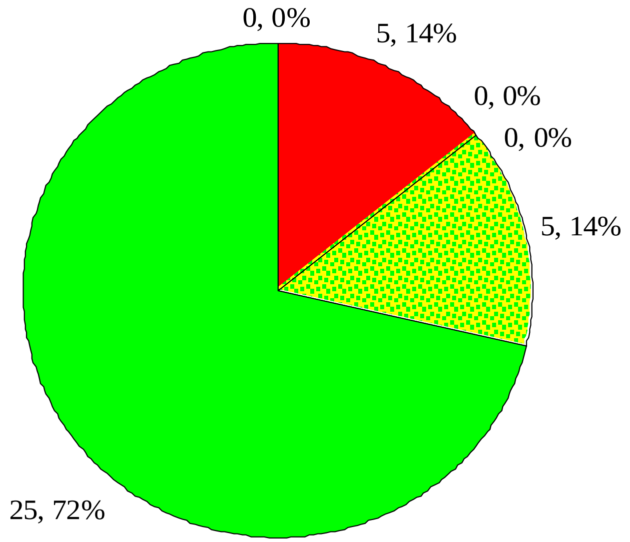

⇒ 14% of variants from situational tree **$S_1 \cdot \Gamma_3$**, which have commanded flight path angle (during initial phase of climb) more than 12^o, exhibit danger. Note also how, for example, event **E_7**: ‘altitude 120 m’ changes its location in IFSS due to θ_{G1}.

$S_1 \cdot \Gamma_3$ Normal Takeoff. Forward C.G. Location. Variations/ Errors Of Selection of Commanded Flight Path Angles (Initial And 2nd Phases Of Climb) And Flaps-up Start Altitude

S_1: Normal takeoff, steering commanded flight path and bank angles during initial climb

$$\Gamma_3 = \Phi_1 \times (\Phi_7 + \Phi_8) \times \Phi_6 \equiv \bar{x}_{CG} \times (\theta_{G1} + \theta_{G2}) \times H_{FL}\ (\bar{x}_{CG} = \bar{x}_{CG\min})$$

FSW

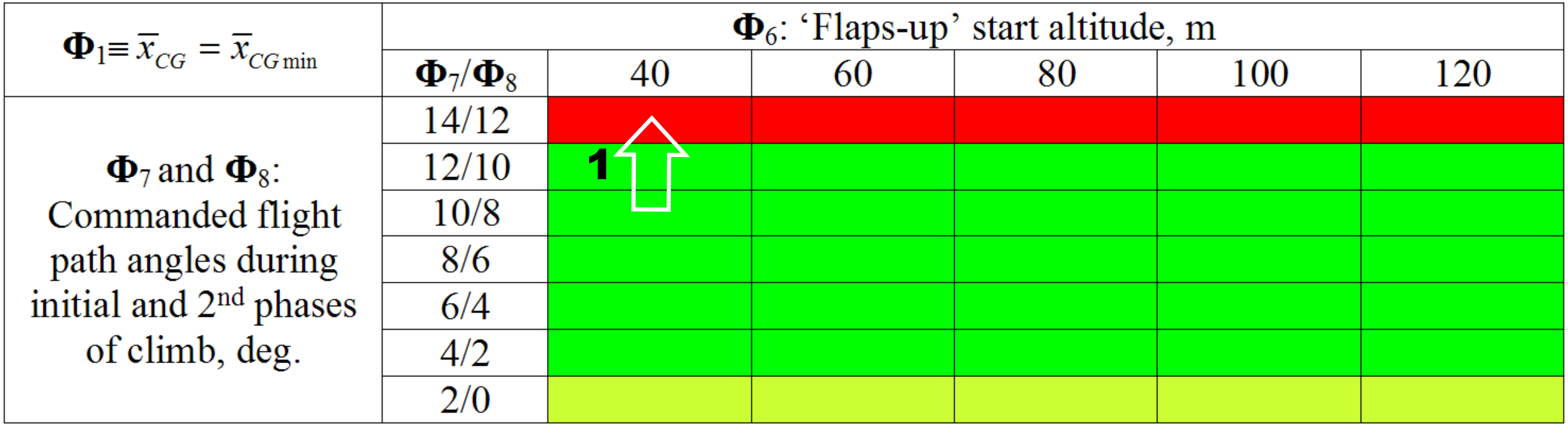

$\Phi_1 \equiv \bar{x}_{CG} = \bar{x}_{CG\min}$	Φ_6: 'Flaps-up' start altitude, m					
	Φ_7/Φ_8	40	60	80	100	120
Φ_7 and Φ_8: Commanded flight path angles during initial and 2nd phases of climb, deg.	14/12	🟥	🟥	🟥	🟥	🟥
	12/10	🟩	🟩	🟩	🟩	🟩
	10/8	🟩	🟩	🟩	🟩	🟩
	8/6	🟩	🟩	🟩	🟩	🟩
	6/4	🟩	🟩	🟩	🟩	🟩
	4/2	🟩	🟩	🟩	🟩	🟩
	2/0	🟨	🟨	🟨	🟨	🟨

⇒ For composition **$S_1 \cdot \Gamma_3$**, sharp transitions (**1**) from safe situations to unsafe ones are observed at commanded flight path angles θ_{G1}/θ_{G2}>12/10° for all values of H_{FL}. Owing to high thrust-to-weight ratio, errors in selection of flaps-up start altitude do not worsen the aircraft's flight safety performance, provided (NB) that other conditions of scenario **S_1** are preserved.

$S_3 \cdot \Gamma_5$ Continued Takeoff. Left-hand Engine Out At V_{EF}=150 km/h. Variations/ Errors of Selection of Commanded Flight Path Angles During Initial And 2nd Phases

IFSS

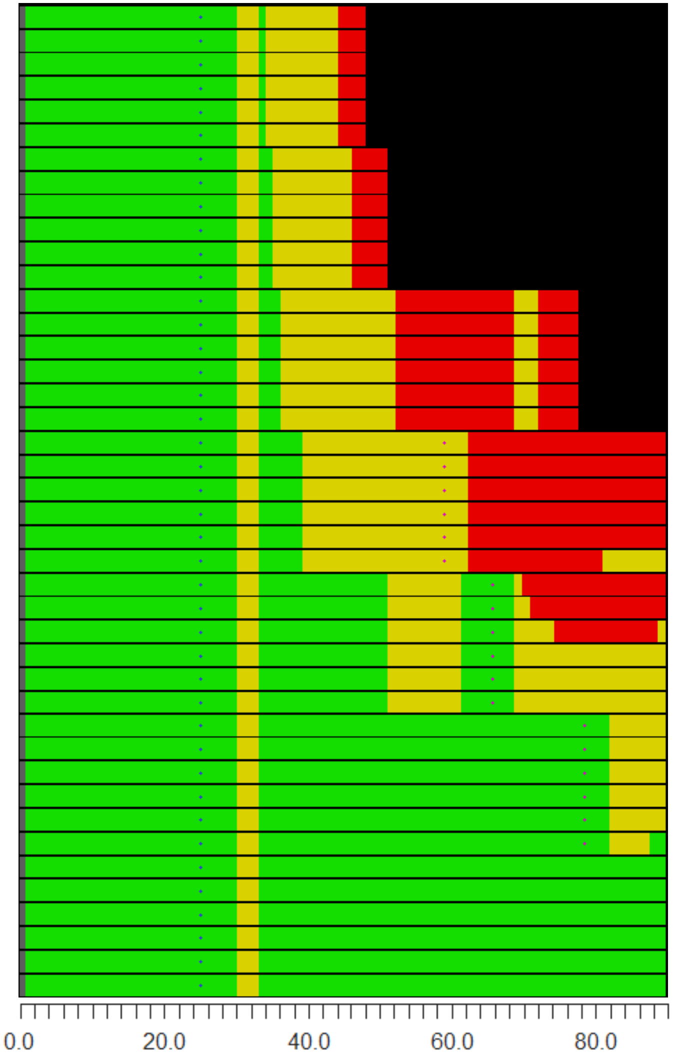

#	θ_{G1}	θ_{G2}
542	7.00	5.00
541	7.00	4.00
540	7.00	3.00
539	7.00	2.00
538	7.00	1.00
537	7.00	0.00
536	6.00	5.00
535	6.00	4.00
534	6.00	3.00
533	6.00	2.00
532	6.00	1.00
531	6.00	0.00
530	5.00	5.00
529	5.00	4.00
528	5.00	3.00
527	5.00	2.00
526	5.00	1.00
525	5.00	0.00
524	4.00	5.00
523	4.00	4.00
522	4.00	3.00
521	4.00	2.00
520	4.00	1.00
519	4.00	0.00
518	3.00	5.00
517	3.00	4.00
516	3.00	3.00
515	3.00	2.00
514	3.00	1.00
513	3.00	0.00
512	2.00	5.00
511	2.00	4.00
510	2.00	3.00
509	2.00	2.00
508	2.00	1.00
507	2.00	0.00
506	1.00	5.00
505	1.00	4.00
504	1.00	3.00
503	1.00	2.00
502	1.00	1.00
501	1.00	0.00

Safety Chances Pie Chart

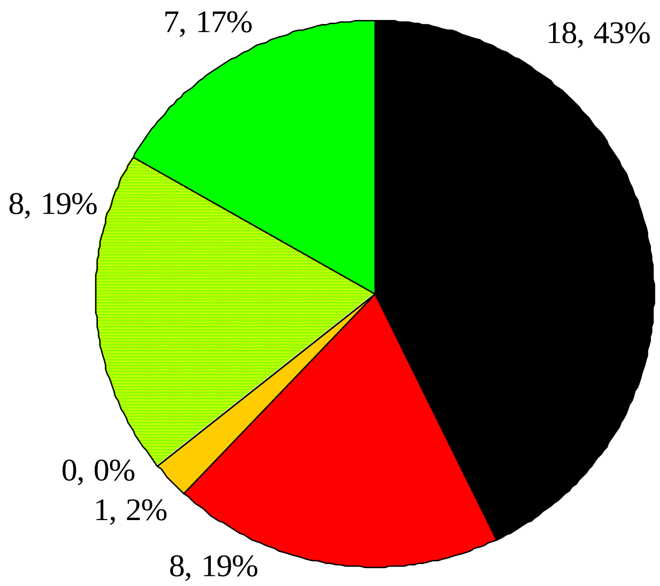

⇒ If left-hand engine fails during ground-roll (at V_{EF}=150 km/h) takeoff safety cannot be secured at commanded flight path angle $\theta_{G1} \geq 5^o$ (during initial phase of climb). For examined domain of operational factors, share of safe situations is 36%.

$S_3 \cdot \Gamma_5$ Continued Takeoff. Left-hand Engine Out At V_{EF}=150 km/h. Variations/ Errors of Selection of Commanded Flight Path Angles During Initial And 2nd Phases

S_3: Continued takeoff (left-hand engine out at given V_{EF}), steering commanded flight path and bank angles during initial climb

$\boldsymbol{\Gamma}_5 = \boldsymbol{\Phi}_{13}\times\boldsymbol{\Phi}_7\times\boldsymbol{\Phi}_8 \equiv \zeta_{LHE}\times\theta_{G1}\times\theta_{G2}$ (V_{EF}=150 км/ч)

FSW

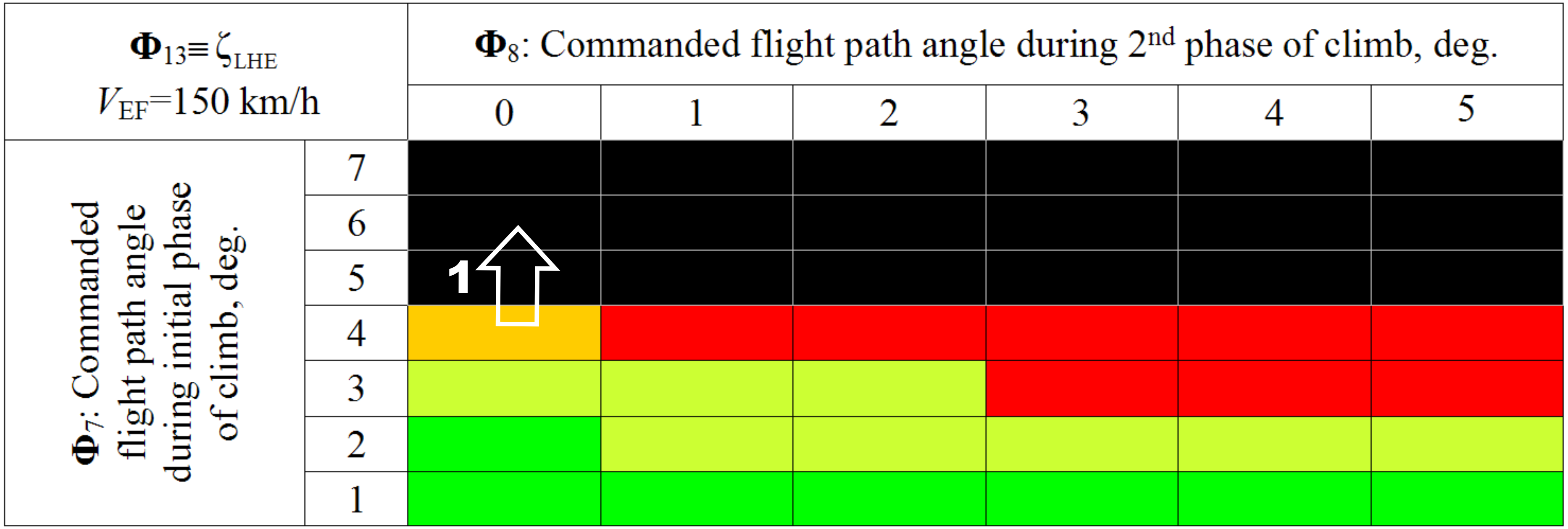

$\boldsymbol{\Phi}_{13}\equiv\zeta_{LHE}$ V_{EF}=150 km/h		$\boldsymbol{\Phi}_8$: Commanded flight path angle during 2nd phase of climb, deg.					
		0	1	2	3	4	5
$\boldsymbol{\Phi}_7$: Commanded flight path angle during initial phase of climb, deg.	7	⬛	⬛	⬛	⬛	⬛	⬛
	6	⬛	⬛	⬛	⬛	⬛	⬛
	5	⬛ **1** ⇧	⬛	⬛	⬛	⬛	⬛
	4	🟧	🟥	🟥	🟥	🟥	🟥
	3	🟨	🟨	🟨	🟥	🟥	🟥
	2	🟩	🟨	🟨	🟨	🟨	🟨
	1	🟩	🟩	🟩	🟩	🟩	🟩

⇒ Left-hand engine failure during ground-roll decreases the limit of flight path angle admissible in initial climb to 2°…4° compared to θ_{G1}=10° …12° in composition **$S_1 \cdot \Gamma_3$**. 'Precipice' type transitions (**1**) are observed at θ_{G2}=0°. 'Abyss' type states are likely to occur at flight path angles θ_{G1}>4° (initial climb) for any θ_{G2} (2nd phase of climb).

$S_4 \cdot \Gamma_6$ Normal Takeoff. Variations Of Windshear Intensity And Errors of Selection of Flaps-up Start Altitude

S_4: Normal takeoff under windshear conditions, steering commanded flight path and bank angles during initial climb

$$\boldsymbol{\Gamma}_6 = \boldsymbol{\Phi}_9 \times \boldsymbol{\Phi}_6 \equiv k_W \times H_{FL}$$

FSW

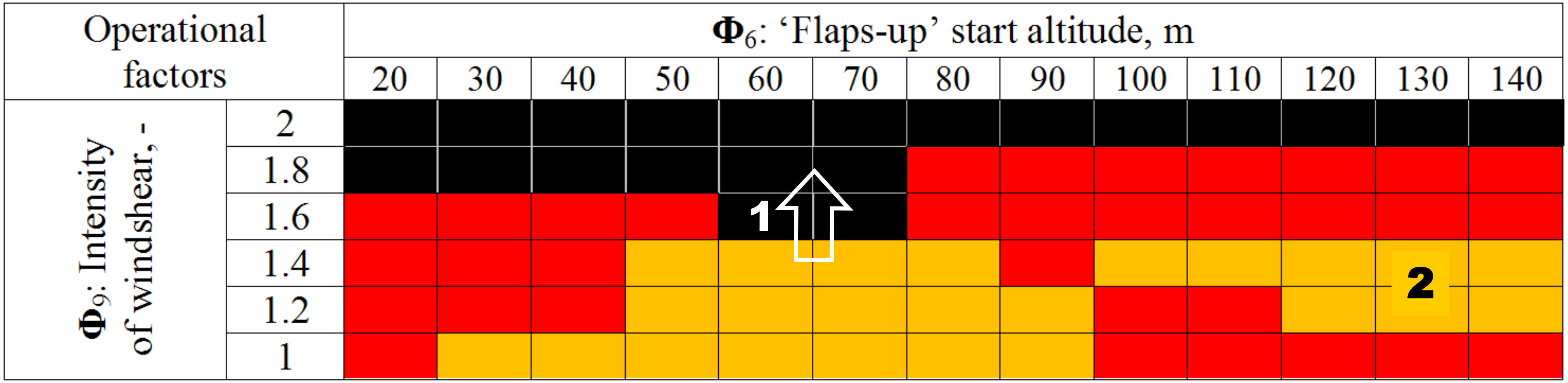

Operational factors		Φ_6: ‘Flaps-up’ start altitude, m												
		20	30	40	50	60	70	80	90	100	110	120	130	140
Φ_9: Intensity of windshear, -	2	⬛	⬛	⬛	⬛	⬛	⬛	⬛	⬛	⬛	⬛	⬛	⬛	⬛
	1.8	⬛	⬛	⬛	⬛	⬛	⬛	🟥	🟥	🟥	🟥	🟥	🟥	🟥
	1.6	🟥	🟥	🟥	🟥	⬛	⬛	🟥	🟥	🟥	🟥	🟥	🟥	🟥
	1.4	🟥	🟥	🟥	🟧	🟧	🟧	🟧	🟥	🟧	🟧	🟧	🟧	🟧
	1.2	🟥	🟥	🟥	🟧	🟧	🟧	🟧	🟧	🟥	🟥	🟧	🟧	🟧
	1	🟥	🟧	🟧	🟧	🟧	🟧	🟧	🟧	🟥	🟥	🟥	🟥	🟥

⇒ In scenario **S_4** we have $\theta_{G1}/\theta_{G2}=8^o/8^o$. If ‘strong’ or worse windshear is expected ($k_W \geq 1$) takeoff is prohibited. In order to evaluate possibility of safe outcomes at $k_W<1$ it is expedient to expand Flight Safety Window downward. If windshear intensity increases from ‘very strong’ ($k_W>1.4$) to ‘hurricane’ ($k_W=2$), ‘precipice’ type transitions (**1**) are most likely to occur at flaps-up start altitude $H_{FL} \in [60; 70]$ м. If aircraft unintentionally enters a zone of ‘very strong’ windshear ($k_W=1.2 \ldots 1.6$) flaps must be retracted as late as possible to stay within ‘orange’ zone (**2**).

$S_4 \cdot \Gamma_7$ Normal Takeoff. Forward C.G. Location. Variations Of Windshear Intensity And Commanded Flight Path Angles (During Initial And 2nd Phases)

S_4: Normal takeoff under windshear conditions, steering commanded flight path and bank angles during initial climb

$$\Gamma_7 = \Phi_1 \times \Phi_9 \times (\Phi_7 + \Phi_8) \equiv \bar{x}_{CG} \times k_W \times (\theta_{G1} + \theta_{G2}) \;\; (\bar{x}_{CG} = \bar{x}_{CG\min})$$

FSW

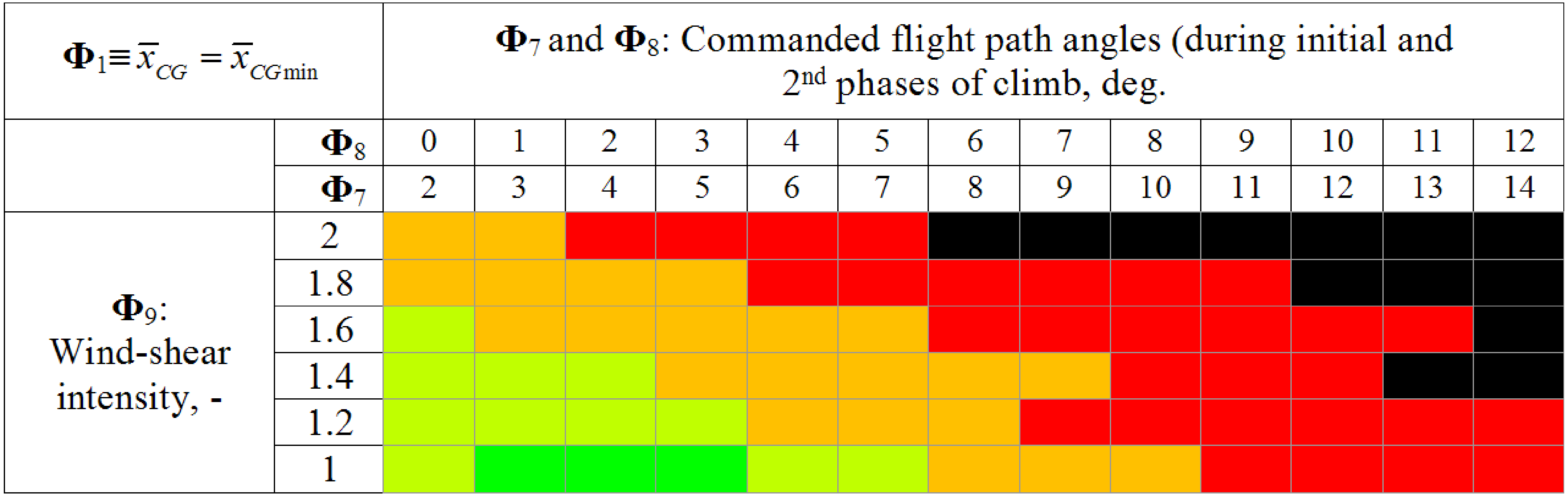

$\Phi_1 \equiv \bar{x}_{CG} = \bar{x}_{CG\min}$		Φ_7 and Φ_8: Commanded flight path angles (during initial and 2nd phases of climb, deg.												
	Φ_8	0	1	2	3	4	5	6	7	8	9	10	11	12
	Φ_7	2	3	4	5	6	7	8	9	10	11	12	13	14
Φ_9: Wind-shear intensity, -	2	🟧	🟧	🟥	🟥	🟥	🟥	⬛	⬛	⬛	⬛	⬛	⬛	⬛
	1.8	🟧	🟧	🟧	🟧	🟥	🟥	🟥	🟥	🟥	🟥	⬛	⬛	⬛
	1.6	🟨	🟧	🟧	🟧	🟧	🟧	🟥	🟥	🟥	🟥	🟥	🟥	⬛
	1.4	🟨	🟨	🟨	🟧	🟧	🟧	🟧	🟧	🟥	🟥	🟥	⬛	⬛
	1.2	🟨	🟨	🟨	🟨	🟧	🟧	🟧	🟥	🟥	🟥	🟥	🟥	🟥
	1	🟨	🟩	🟩	🟩	🟨	🟨	🟧	🟧	🟧	🟥	🟥	🟥	🟥

$\Rightarrow$ For composition **$S_4 \cdot \Gamma_7$** main objects of safety 'topology' are: small green 'valley' (at left lower corner), orange 'slope', extensive red 'hill' adjacent to black 'abyss' (at right upper corner). At takeoff under 'strong' and 'very strong' windshear conditions ($1 < k_W \leq 1.6$): maximum safety is achieved at $\theta_{G1}/\theta_{G2} = 5^o/3^o$; it is prohibited to climb at $\theta_{G1}/\theta_{G2} > 7^o/5^o$; irreversible transitions are likely at $\theta_{G1} \geq 12^o$.

$S_5 \cdot \Gamma_{10}$ Continued Takeoff. Left-hand Engine Out At V_{EF}. Variations Of Left-hand Engine Out Speed And Crosswind Velocity

S_5: Continued takeoff (left-hand engine out at V_{EF}), under cross-wind conditions, steering commanded flight path and bank angles during initial climb

$\mathbf{\Gamma}_{10} = \mathbf{\Phi}_{13} \times \mathbf{\Phi}_{12} \times \mathbf{\Phi}_4 \equiv \zeta_{LHE} \times V_{EF} \times W_{yg}$

FSW

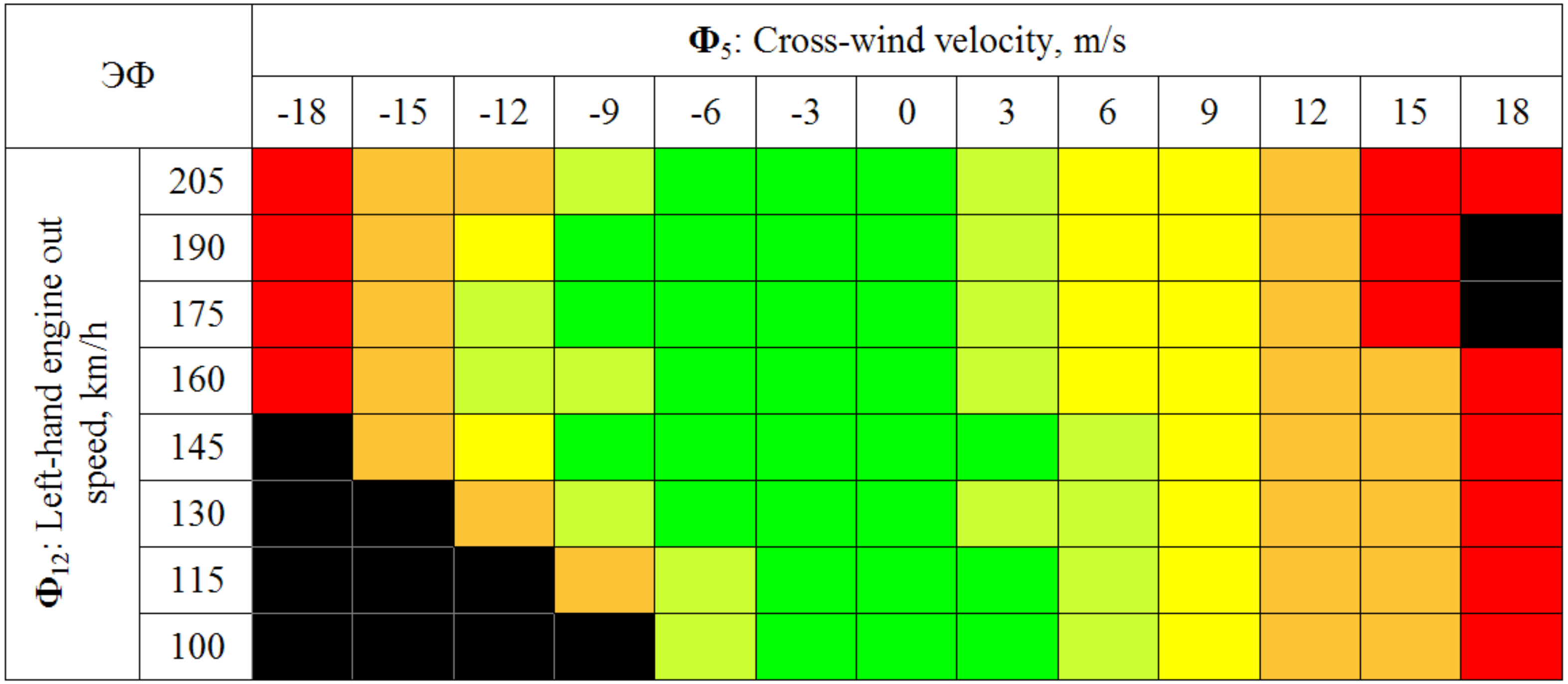

ЭФ		**Φ_5**: Cross-wind velocity, m/s												
		-18	-15	-12	-9	-6	-3	0	3	6	9	12	15	18
Φ_{12}: Left-hand engine out speed, km/h	205	🟥	🟧	🟧	▨	🟩	🟩	🟩	▨	🟨	🟨	🟧	🟥	🟥
	190	🟥	🟧	🟨	🟩	🟩	🟩	🟩	▨	🟨	🟨	🟧	🟥	⬛
	175	🟥	🟧	▨	🟩	🟩	🟩	🟩	▨	🟨	🟨	🟧	🟥	⬛
	160	🟥	🟧	▨	▨	🟩	🟩	🟩	▨	🟨	🟨	🟧	🟧	🟥
	145	⬛	🟧	🟨	🟩	🟩	🟩	🟩	🟩	▨	🟨	🟧	🟧	🟥
	130	⬛	⬛	🟧	▨	🟩	🟩	🟩	▨	▨	🟨	🟧	🟧	🟥
	115	⬛	⬛	⬛	🟧	▨	🟩	🟩	🟩	▨	🟨	🟧	🟧	🟥
	100	⬛	⬛	⬛	⬛	▨	🟩	🟩	🟩	▨	🟨	🟧	🟧	🟥

⇒ This Flight Safety Window has central green ‘valley’ and two side red ‘hills’. Adjacent to left ‘hill’ is a potentially catastrophic ‘abyss’ located at lower left corner. It is created at small and medium values of V_{EF} and is linked to ‘valley’ by ‘precipice’ type transitions. Small ‘abyss’ is also revealed at crosswind velocity of ~18 m/s and $V_{EF} \in [175; 190]$ km/h.

Graphic Implementation Options Of Flight Safety Window ($S_5 \cdot \Gamma_{10}$ Example)

1

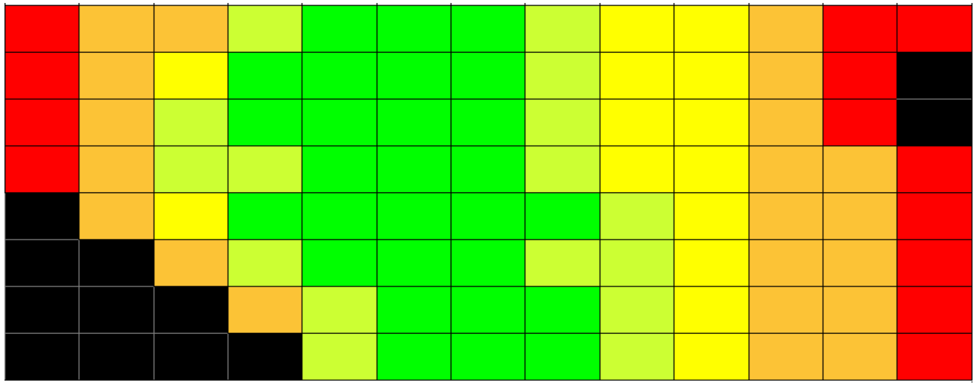

2

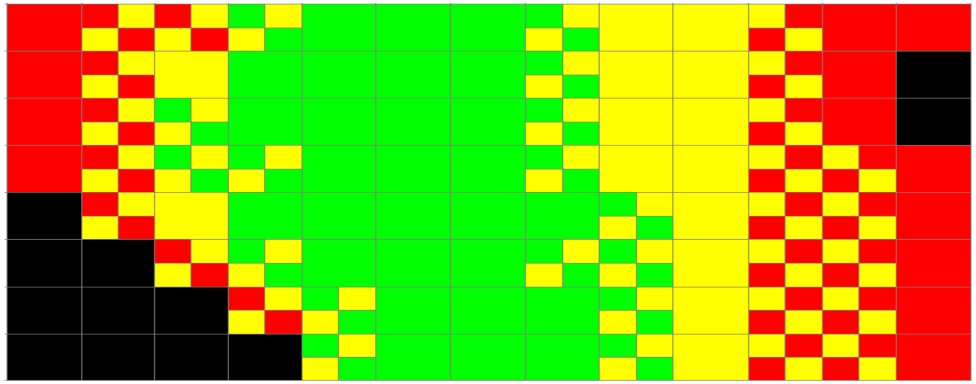

3

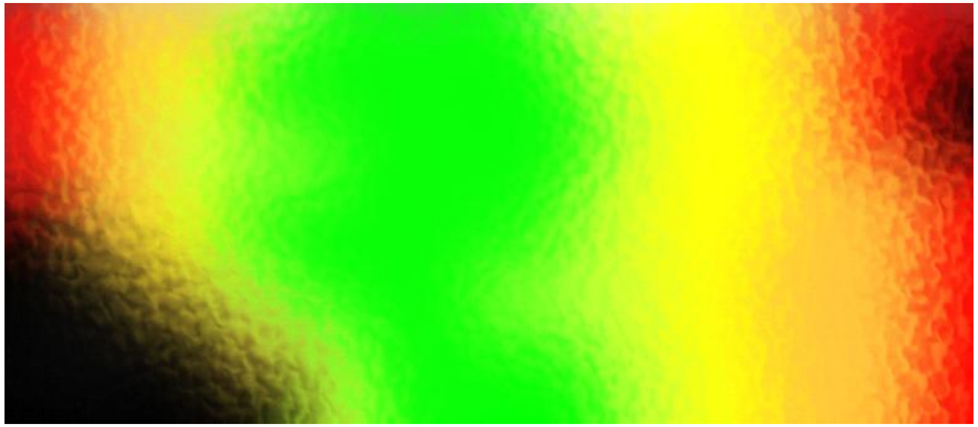

⇒ Option **1** adequately maps complex safety ‘topology’. It is quite sufficient for manual/ automatic decision making in flight for flight safety protection.

⇒ Option **2** does not meet ergonomic criteria for optimal pilot-vehicle interface.

⇒ Option **3** would be close to an ideal onboard solution. However, it can only be used if sufficient computer resources are available.

<u>Legend</u>:

1 VATES v.7 output (six-color Safety Palette)
2 Mosaic (four-color) Safety Palette
3 Option **1** after special filtering

$S_1 \cdot \Gamma_{11}$ Normal Takeoff. Variations/ Errors In Selection Of Commanded Flight Path And Bank Angles (During Initial Phase Of Climb)

S_1: Normal takeoff, steering commanded flight path and bank angles during initial climb

$$\Gamma_{11} = \mathbf{\Phi}_7 \times \mathbf{\Phi}_{11} \equiv \theta_{G1} \times \gamma_G$$

FSW

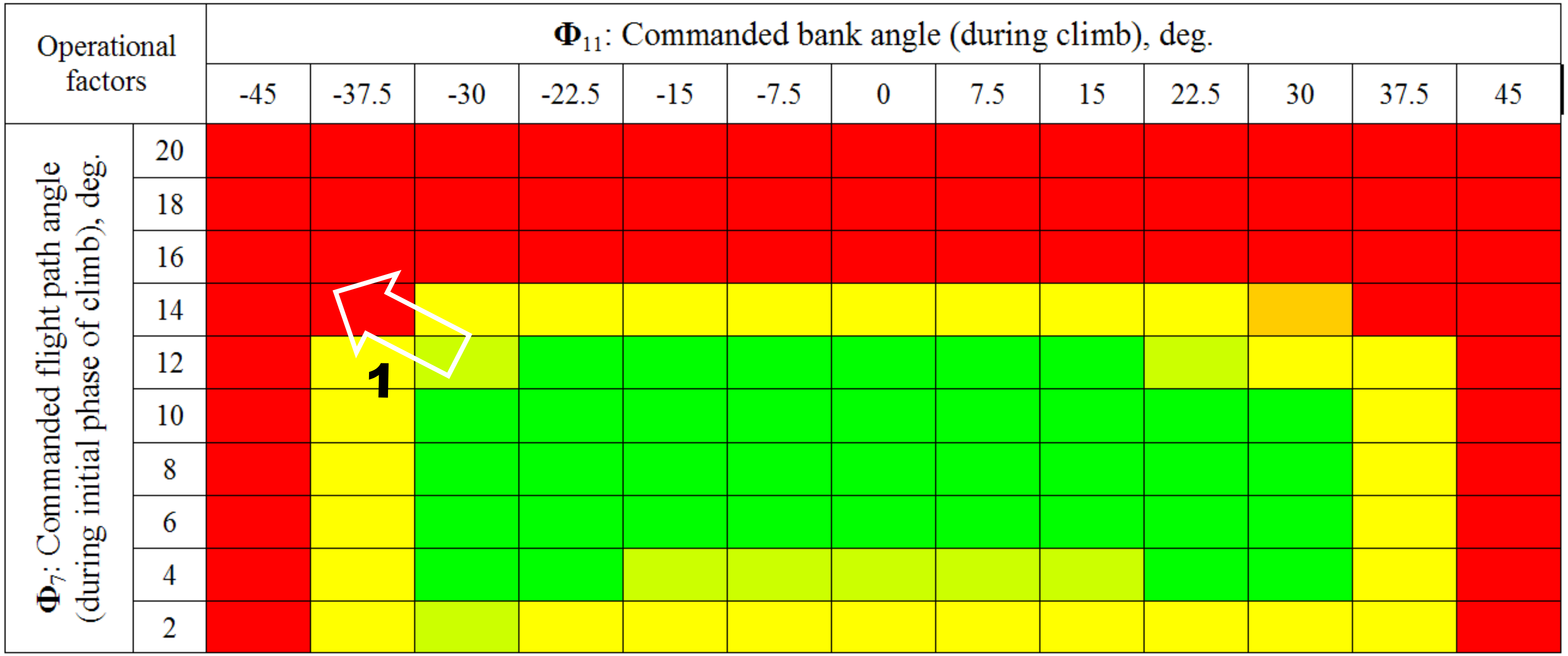

Operational factors		$\mathbf{\Phi}_{11}$: Commanded bank angle (during climb), deg.												
		-45	-37.5	-30	-22.5	-15	-7.5	0	7.5	15	22.5	30	37.5	45
$\mathbf{\Phi}_7$: Commanded flight path angle (during initial phase of climb), deg.	20	🟥	🟥	🟥	🟥	🟥	🟥	🟥	🟥	🟥	🟥	🟥	🟥	🟥
	18	🟥	🟥	🟥	🟥	🟥	🟥	🟥	🟥	🟥	🟥	🟥	🟥	🟥
	16	🟥	🟥	🟥	🟥	🟥	🟥	🟥	🟥	🟥	🟥	🟥	🟥	🟥
	14	🟥	🟥	🟨	🟨	🟨	🟨	🟨	🟨	🟨	🟨	🟧	🟥	🟥
	12	🟥	🟨	▨	🟩	🟩	🟩	🟩	🟩	🟩	▨	🟨	🟨	🟥
	10	🟥	🟨	🟩	🟩	🟩	🟩	🟩	🟩	🟩	🟩	🟩	🟨	🟥
	8	🟥	🟨	🟩	🟩	🟩	🟩	🟩	🟩	🟩	🟩	🟩	🟨	🟥
	6	🟥	🟨	🟩	🟩	🟩	🟩	🟩	🟩	🟩	🟩	🟩	🟨	🟥
	4	🟥	🟨	🟩	🟩	▨	▨	▨	▨	▨	🟩	🟩	🟨	🟥
	2	🟥	🟨	▨	🟨	🟨	🟨	🟨	🟨	🟨	🟨	🟨	🟨	🟥

⇒ This Flight Safety Window has a potentially dangerous ‘corner’ corresponding to (θ_{G1}, γ_G) ≅ (12°…14°, -30°…-37.5°). Sharp transition (**1**) of states from safe (‘green’) to dangerous (‘red’) zone is possible (Cat. **I**→**IV**), bypassing interim zones (Cat. **II**, **III**). Flight at such ‘corners’ requires enhanced attention and accurate piloting from pilot.

$S_4 \cdot \Gamma_{13}$ Normal Takeoff. ‘Very’ Strong Windshear. Variations /Errors Of Selection Of Commanded Flight Path And Bank Angles in Climb

IFSS

#	θ_{G1}	γ_G
3265	10.00	45.00
3264	10.00	37.50
3263	10.00	30.00
3262	10.00	22.50
3261	10.00	15.00
3260	10.00	7.50
3259	10.00	0.00
3258	10.00	-7.50
3257	10.00	-15.00
3256	10.00	-22.50
3255	10.00	-30.00
3254	10.00	-37.50
3253	10.00	-45.00
3252	8.00	45.00
3251	8.00	37.50
3250	8.00	30.00
3249	8.00	22.50
3248	8.00	15.00
3247	8.00	7.50
3246	8.00	0.00
3245	8.00	-7.50
3244	8.00	-15.00
3243	8.00	-22.50
3242	8.00	-30.00
3241	8.00	-37.50
3240	8.00	-45.00
3239	6.00	45.00
3238	6.00	37.50
3237	6.00	30.00
3236	6.00	22.50
3235	6.00	15.00
3234	6.00	7.50
3233	6.00	0.00
3232	6.00	-7.50
3231	6.00	-15.00
3230	6.00	-22.50
3229	6.00	-30.00
3228	6.00	-37.50
3227	6.00	-45.00
3226	4.00	45.00
3225	4.00	37.50
3224	4.00	30.00
3223	4.00	22.50
3222	4.00	15.00
3221	4.00	7.50
3220	4.00	0.00
3219	4.00	-7.50
3218	4.00	-15.00
3217	4.00	-22.50
3216	4.00	-30.00
3215	4.00	-37.50
3214	4.00	-45.00
3213	2.00	45.00
3212	2.00	37.50
3211	2.00	30.00
3210	2.00	22.50
3209	2.00	15.00
3208	2.00	7.50
3207	2.00	0.00
3206	2.00	-7.50
3205	2.00	-15.00
3204	2.00	-22.50
3203	2.00	-30.00
3202	2.00	-37.50
3201	2.00	-45.00

IFSS

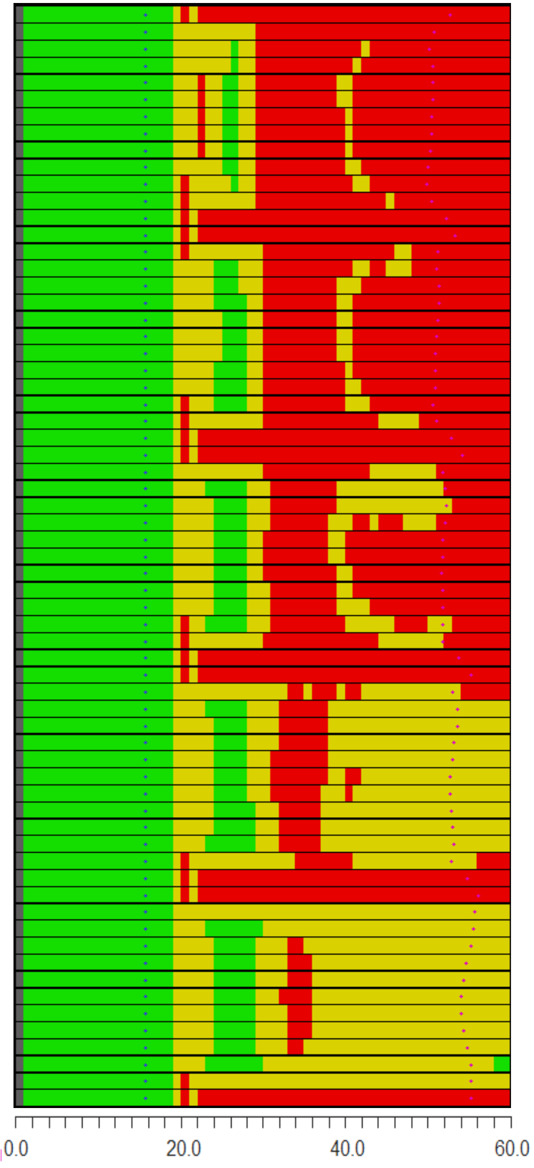

#	θ_{G1}	γ_G
3330	20.00	45.00
3329	20.00	37.50
3328	20.00	30.00
3327	20.00	22.50
3326	20.00	15.00
3325	20.00	7.50
3324	20.00	0.00
3323	20.00	-7.50
3322	20.00	-15.00
3321	20.00	-22.50
3320	20.00	-30.00
3319	20.00	-37.50
3318	20.00	-45.00
3317	18.00	45.00
3316	18.00	37.50
3315	18.00	30.00
3314	18.00	22.50
3313	18.00	15.00
3312	18.00	7.50
3311	18.00	0.00
3310	18.00	-7.50
3309	18.00	-15.00
3308	18.00	-22.50
3307	18.00	-30.00
3306	18.00	-37.50
3305	18.00	-45.00
3304	16.00	45.00
3303	16.00	37.50
3302	16.00	30.00
3301	16.00	22.50
3300	16.00	15.00
3299	16.00	7.50
3298	16.00	0.00
3297	16.00	-7.50
3296	16.00	-15.00
3295	16.00	-22.50
3294	16.00	-30.00
3293	16.00	-37.50
3292	16.00	-45.00
3291	14.00	45.00
3290	14.00	37.50
3289	14.00	30.00
3288	14.00	22.50
3287	14.00	15.00
3286	14.00	7.50
3285	14.00	0.00
3284	14.00	-7.50
3283	14.00	-15.00
3282	14.00	-22.50
3281	14.00	-30.00
3280	14.00	-37.50
3279	14.00	-45.00
3278	12.00	45.00
3277	12.00	37.50
3276	12.00	30.00
3275	12.00	22.50
3274	12.00	15.00
3273	12.00	7.50
3272	12.00	0.00
3271	12.00	-7.50
3270	12.00	-15.00
3269	12.00	-22.50
3268	12.00	-30.00
3267	12.00	-37.50
3266	12.00	-45.00

Safety Chances Pie Chart

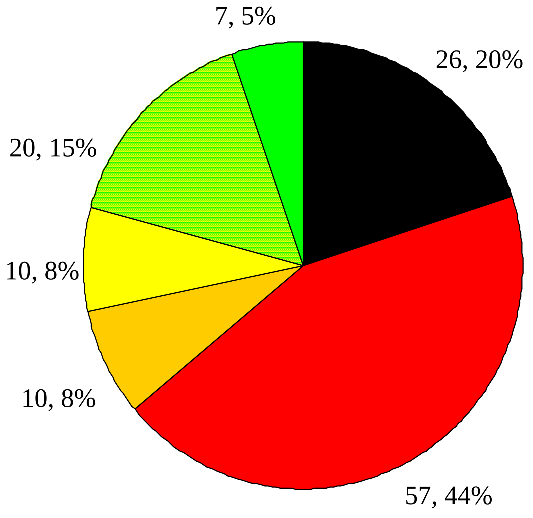

⇒ ‘Very strong’ wind-shear may worsen flight safety ‘topology’ of takeoff catastrophically at small values of commanded flight path angle $\theta_{G1} \le 4^o$.

$S_4 \cdot \Gamma_{13}$ Normal Takeoff. 'Very' Strong Windshear. Variations /Errors Of Selection Of Commanded Flight Path And Bank Angles in Climb

S_4: Normal takeoff under windshear conditions, steering commanded flight path and bank angles during initial climb

$\mathbf{\Gamma}_{13} = \mathbf{\Phi}_9 \times \mathbf{\Phi}_7 \times \mathbf{\Phi}_{11} \equiv k_W \times \theta_{G1} \times \gamma_G \; (k_W=1.5)$

FSW

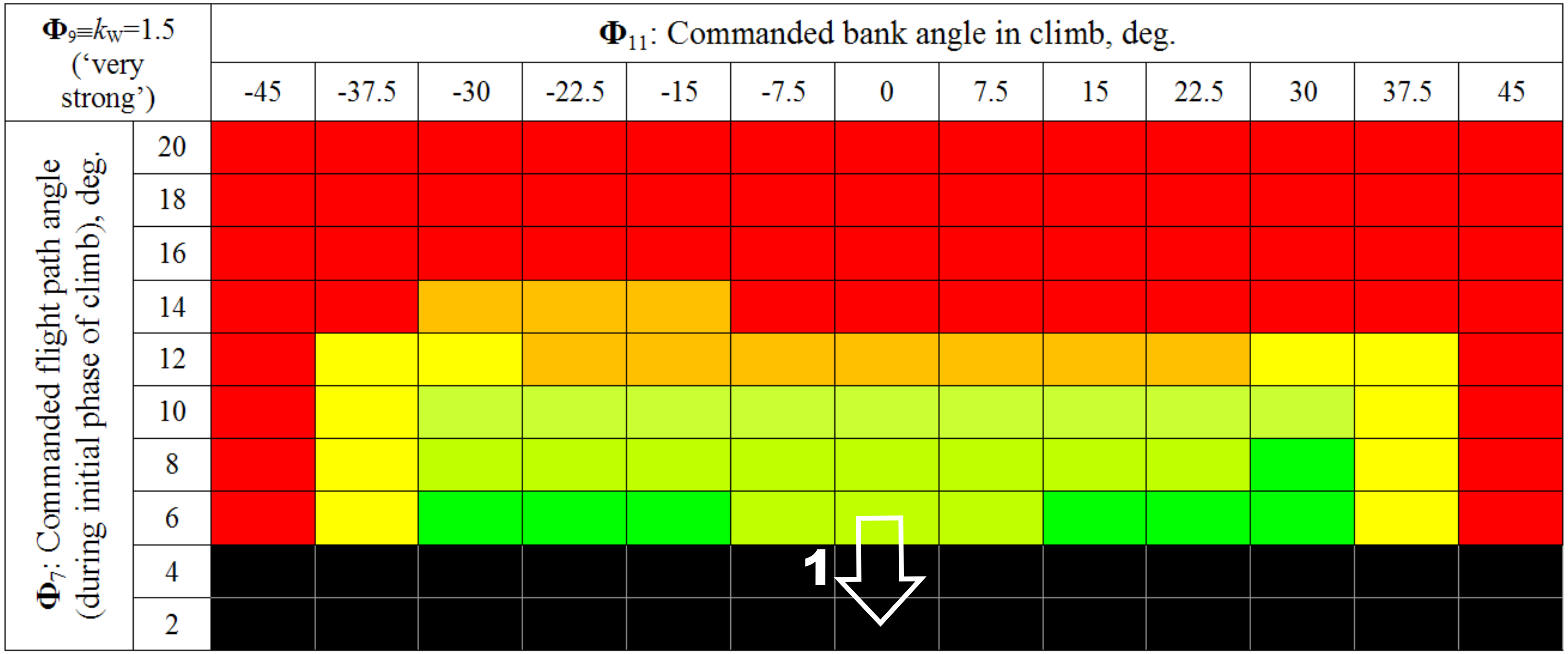

$\mathbf{\Phi}_9 \equiv k_W=1.5$ ('very strong')		$\mathbf{\Phi}_{11}$: Commanded bank angle in climb, deg.												
		-45	-37.5	-30	-22.5	-15	-7.5	0	7.5	15	22.5	30	37.5	45
$\mathbf{\Phi}_7$: Commanded flight path angle (during initial phase of climb), deg.	20	🟥	🟥	🟥	🟥	🟥	🟥	🟥	🟥	🟥	🟥	🟥	🟥	🟥
	18	🟥	🟥	🟥	🟥	🟥	🟥	🟥	🟥	🟥	🟥	🟥	🟥	🟥
	16	🟥	🟥	🟥	🟥	🟥	🟥	🟥	🟥	🟥	🟥	🟥	🟥	🟥
	14	🟥	🟥	🟧	🟧	🟧	🟥	🟥	🟥	🟥	🟥	🟥	🟥	🟥
	12	🟥	🟨	🟨	🟧	🟧	🟧	🟧	🟧	🟧	🟧	🟨	🟨	🟥
	10	🟥	🟨	▨	▨	▨	▨	▨	▨	▨	▨	▨	🟨	🟥
	8	🟥	🟨	▨	▨	▨	▨	▨	▨	▨	▨	🟩	🟨	🟥
	6	🟥	🟨	🟩	🟩	🟩	▨	▨	▨	🟩	🟩	🟩	🟨	🟥
	4	⬛	⬛	⬛	⬛	⬛	⬛	⬛	⬛	⬛	⬛	⬛	⬛	⬛
	2	⬛	⬛	⬛	⬛	⬛	⬛	⬛	⬛	⬛	⬛	⬛	⬛	⬛

⇒ Flight safety 'topology' obtained for 'very strong' windshear conditions at small θ_{G1} and any γ_G contains a stable catastrophic 'abyss' (black strip in the bottom) and "precipice' type transitions (**1**). That is, an attempt of initial climb at small values of commanded flight path angle ($2^o…4^o$) inevitably leads the vehicle to a fatal outcome.

Principles of Real-Time Application – 1

Normal Takeoff. Variations of Wind-shear Intensity, Errors/ Variations Of Selection Of Commanded Flight Path And Bank Angles in Initial Climb

Safety Chances Pie Chart and FSW Snapshot Sequence

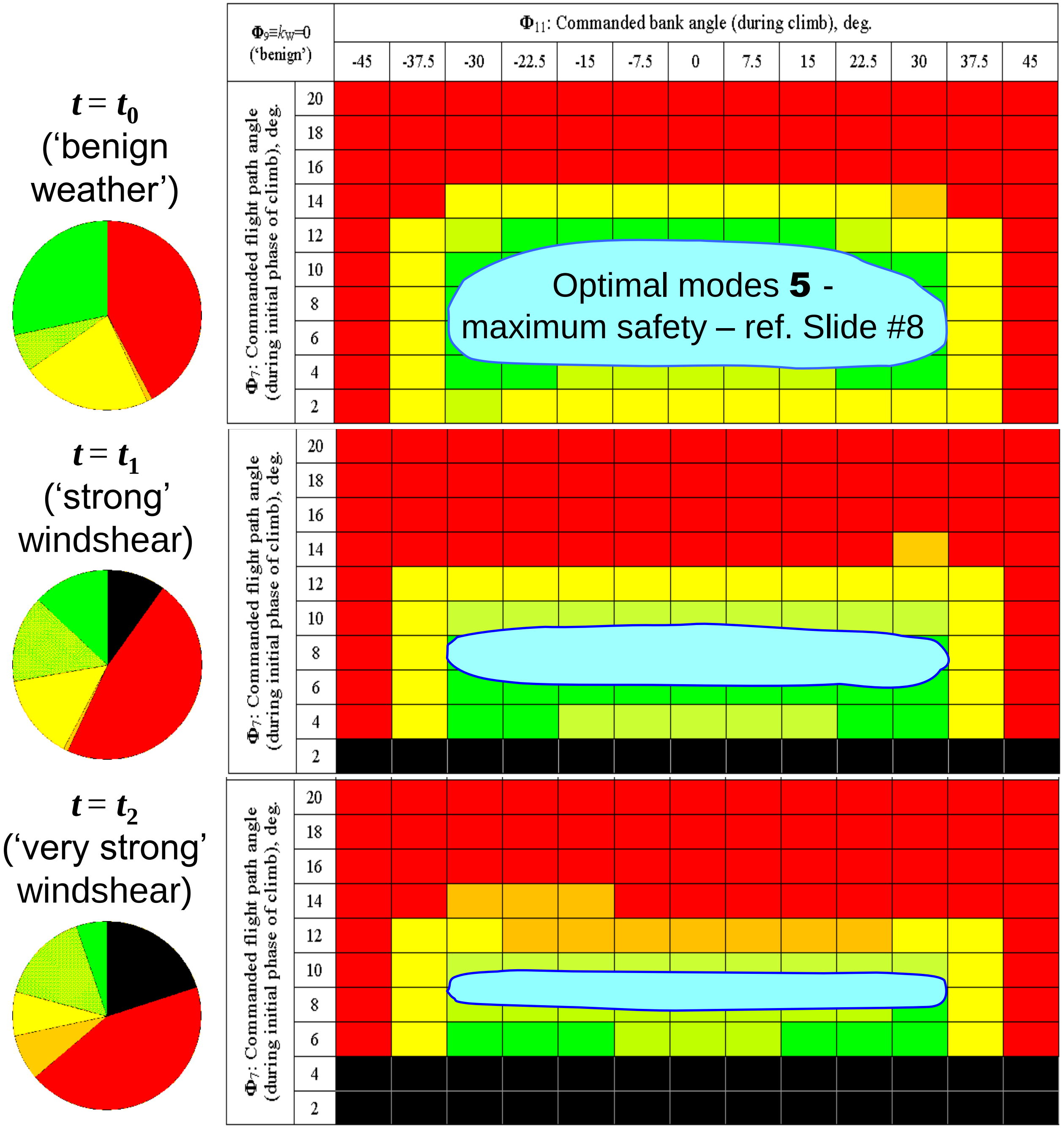

Optimal modes **5** - maximum safety – ref. Slide #8

⇒ The developed safety 'topology' maps, including Flight Safety Window, Safety Chances Pie Chart and other formats, can be used in flight operations. The goal is to monitor complex operational constraints and dynamically adapt piloting tactics under multi-factor conditions in real time, provided that there exist onboard technical means to measure operational factors in real time.

Principles of Real-Time Application – 2

NASA 'Performance Window' Concept

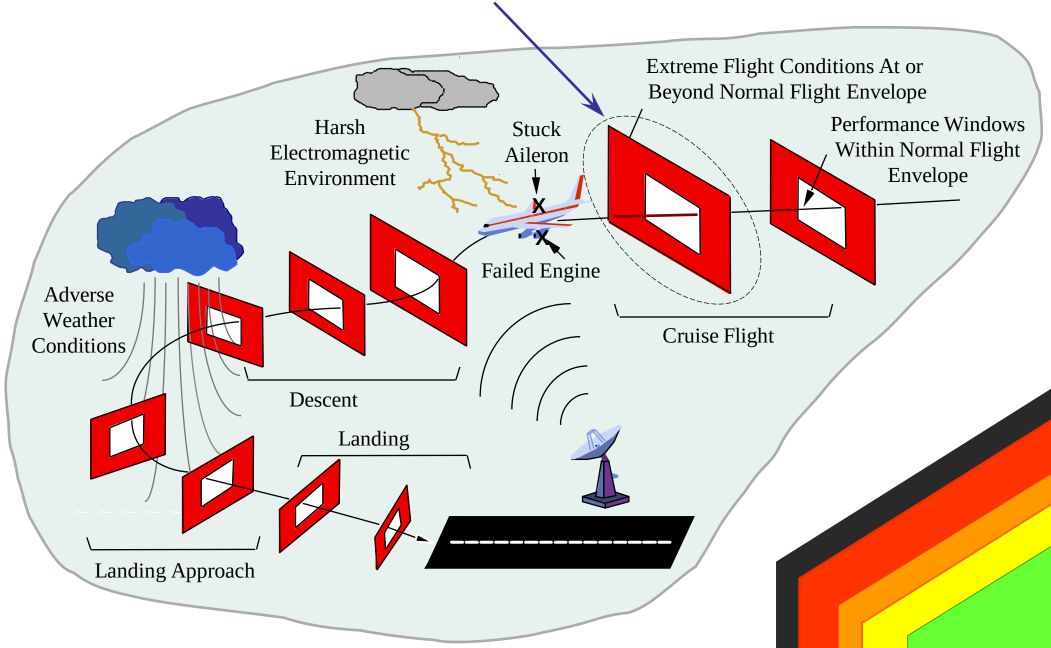

Implementation Techniques

Flight Safety Window

FSD (*)

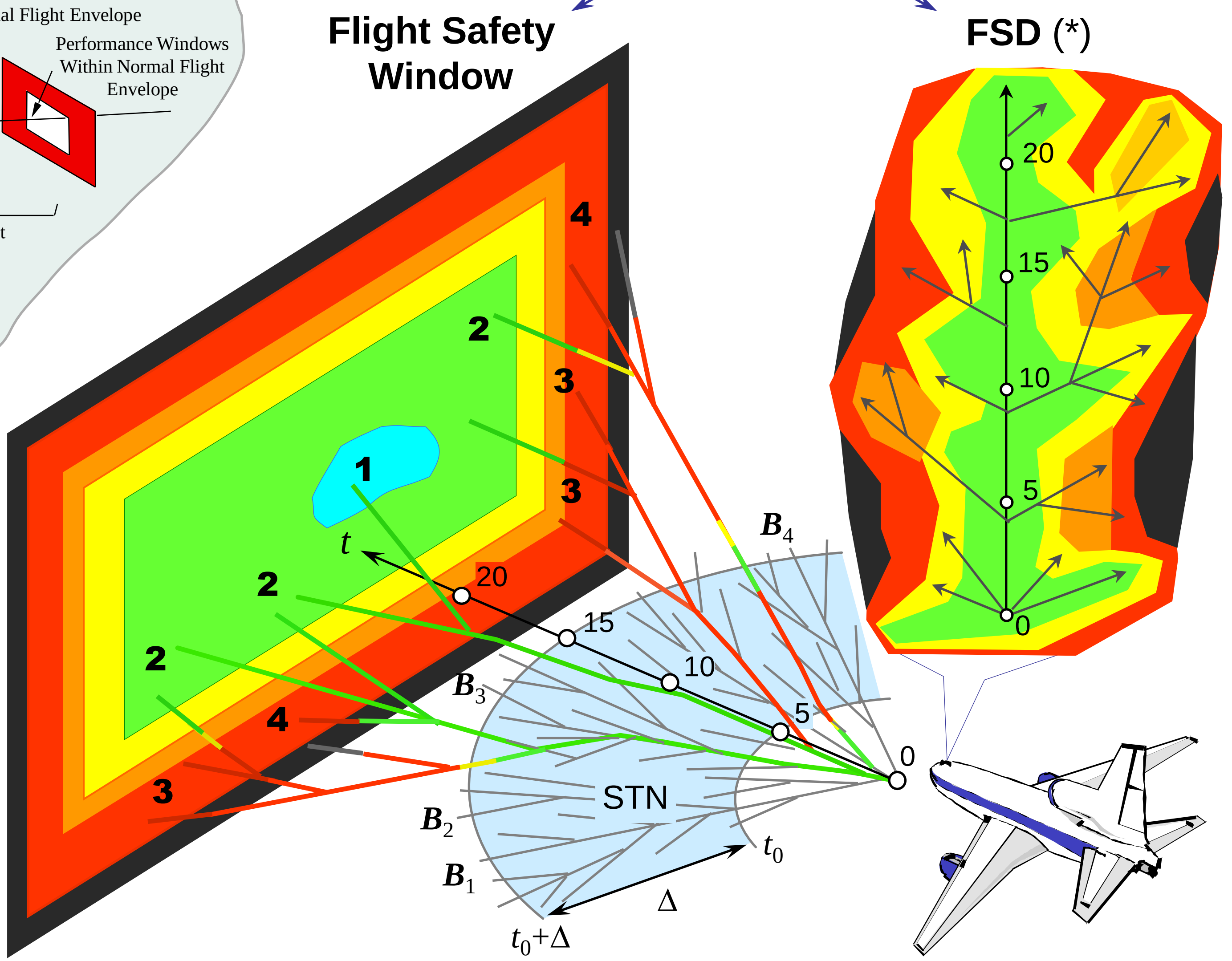

Legend: flight path types: optimal (**1**), safe/recovery (**2**), dangerous (**3**), catastrophic (**4**); t – relative time of forecast, $t \in [t_0;\ t+\Delta]$ (t=0 – current flight time); Δ - depth of forecast; FSD – Flight Situation Display [8]; STN - situational tree-network; examples of situational tree's branches: 'stuck aileron' ($\boldsymbol{B}_1$); 'critical engine failed' ($\boldsymbol{B}_2$); 'adverse weather conditions': 'windshear' ($\boldsymbol{B}_3$), 'heavy rain' ($\boldsymbol{B}_4$); (*) – conceptual layout.

I	II-a	II-b	III	IV	V
🟩	🟩	🟨	🟧	🟥	⬛

⇒ The developed safety 'topology' maps (FSW, FSD) are feasible and affordable implementation techniques of NASA Performance Window concept.

Conclusion - 1

1. A new methodology for testing and evaluation of an aircraft's flight safety performance under complex conditions has been developed, based on design and flight simulation data.

2. A set of two-, three-, and four-factor takeoff situation scenarios that incorporate pilot's errors, onboard systems failures and adverse weather conditions has been examined. A family of flight safety 'topology' maps has been constructed and analyzed for a number of takeoff operational hypotheses. Several characteristic topological objects that can either accelerate or slow down the development of safe or catastrophic outcomes of flight situations under complex conditions have been identified.

3. A technique for the derivation and mapping of aircraft piloting recommendations and operational constraints in multi-factor situations is demonstrated. New principles of pilot training, based on the formation of system-level model-based knowledge of safety 'topology' of a complex flight situation domain, are formulated. Recommendations on aircraft piloting and operational complexity limits at takeoff are proposed. Principles of onboard application of the developed approach for flight safety enhancement/ protection in emergencies are demonstrated.

Conclusion - 2

4. The developed methodology is sensitive to variations of main operational and design factors. Flight Safety Window and other knowledge maps facilitate automated, a ‘bird’s eye’s view’ type analysis of an aircraft’s safety performance for a broad domain of complex (multi-factor) flight situations.

5. The VATES tool is an efficient and affordable source of predictive information on an aircraft’s safety performance under complex operational conditions beginning from early design phases. It takes into account both physics and logics of a given flight situation scenario and its probable/ possible variations (‘what-if neighborhood’).

6. The developed methodology is expedient to apply for studying the following problem classes:

- advanced assessment of combined effects of aerodynamics, control and operational factors on aircraft dynamics and safety performance in design
- knowledge-centered training of line pilots, test pilots and pilot instructors
- development of terrorist-/ fool-proof ‘built-in-safety’ systems
- research into AI based recovery flight control in emergencies (LOC, CFIT, etc.).

Selected Publications

1. Burdun, I.Y., “Prediction of Aircraft Safety Performance in Complex Flight Situations” (Paper 2003-01-2988), *Proc. of the 2003 Advances in Aviation Safety Conference, September 8-12,* 2003, *Montreal, Canada,* SAE, 2003, 18 pp.
2. Burdun, I.Y., “A Technique for Testing and Evaluation of Flight Safety in Complex Situations By Means of ‘Pilot-Aircraft-Operational Environment’ System Model in Design”, *Proc. of VII Russian-Chinese Conference ‘Aerodynamics, Flight Dynamics, Structural Strength’, 12-15 August 2003, TsAGI,* Zhoukovsky, Russia, pp. 84-94.
3. Burdun, I.Y., “Studying Physics and Logics of Complex Flight Situation Domains by Means of VATES Modeling and Simulation Tool”, *2nd Science and Technology Conference “Flight Simulation Technologies and Pilot Training: New Approaches and Goals”, TsAGI, 24-25 April 2003, Zhoukovsky, Moscow Region,* Russia, 2003, 11 pp. (in Russian).
4. Burdun, I.Y., “Introduction to Onboard AI for Flight Safety Enhancement”, *Lecture Course Notes (Chapters 4-7),* Issue 2, Novosibirsk, Russia, 2001, 57 pp. (in Russian).
5. Burdun, I.Y., Schrage, D.P., “Flight Certification and Safety by Design. Introduction of Virtual Testing and Certification”, Course AE 8133, *Lecture Notes; XV-15, HSCT Modeling and Simulation Project Handouts*, School of Aerospace Engineering, Georgia Institute of Techology, Spring/Summer Quarter Academic Year 1998/1999.
6. Burdun, I.Y., Parfentyev, O.M., “Fuzzy Situational Tree-Networks for Intelligent Flight Support”, *Int. Journal of Engineering Applications of Artificial Intelligence (EAAI)*, 12 (1999), pp. 523-541.
7. Schrage, D.P., Calise, A.J., Burdun, I.Y., Pritchett, A., and Rysdyk, R.T., “An Integrated Knowledge-Based Approach to Improving Aircraft Safety”, *White Paper*, School of Aerospace Engineering, Georgia Institute of Technology, USA, Oct. 1998, 20 pp.
8. Burdun, I.Y., “The Intelligent Situational Awareness And Forecasting Environment (The S.A.F.E. Concept): A Case Study” (Paper 981223), *Proc. of 1998 Advances in Flight Safety Conference and Exhibition, April 6-8, 1998, Daytona Beach, FL, USA* (P-321), SAE, 1998, pp.131-144.
9. Burdun, I.Y., “A Method for Accident Reconstruction and Neighborhood Analysis Using an Autonomous Situational Model of Flight and Flight Recorder Data” (Paper 1999-01-1434), *Proc. of the 1999 Advances in Aviation Safety Conference, April 13-15, 1999, Daytona Beach, FL, USA* (P-343), SAE, 1999.
10. Burdun, I.Y., and Parfentyev, O.M., “Analysis of Aerobatic Flight Safety Using Autonomous Modeling and Simulation” (Paper 2000-01-2100), *Proc. of the 2000 Advances in Aviation Safety Conference, April 11-13, 2000, Daytona Beach, FL, USA* (P-355), SAE, 2000, pp. 75-92.
11. Burdun, I.Y., Parfentyev, O.M., “AI Knowledge Model for Self-Organizing Conflict Prevention/Resolution in Close Free-Flight Air Space”, *Proc. Of IEEE Aerospace Applications Conference, Snowmass, Colorado, March 6-13, vol. 2, 1999, USA*, IEEE, 1999, pp. 409-428.
12. Burdun, I.Y., and Mavris, D.N, “A Technique for Testing and Evaluation of Aircraft Flight Performance In Early Design Phases” (Paper 975541), In: *Proc. of the World Aviation Congress (WAC'97), Anaheim, Oct. 1997, CA, USA*, AIAA-SAE, 1997, 13 pp.

Questions?